NASA TN D-417

TECHNICAL NOTE
D-417

INVESTIGATION OF EFFECTS OF ROUGHNESS, SURFACE COOLING, AND SHOCK IMPINGEMENT ON BOUNDARY-LAYER TRANSITION ON A TWO-DIMENSIONAL WING

By K. R. Czarnecki and John R. Sevier, Jr.

Langley Research Center
Langley Field, Va.

NATIONAL AERONAUTICS AND SPACE ADMINISTRATION

WASHINGTON

June 1960

NATIONAL AERONAUTICS AND SPACE ADMINISTRATION

TECHNICAL NOTE D-417

INVESTIGATION OF EFFECTS OF ROUGHNESS, SURFACE COOLING, AND SHOCK IMPINGEMENT ON BOUNDARY-LAYER TRANSITION ON A TWO-DIMENSIONAL WING

By K. R. Czarnecki and John R. Sevier, Jr.

SUMMARY

An investigation has been made to determine the effects of single-element surface roughness, surface cooling, and shock impingement on boundary-layer transition on a two-dimensional wing. The wing had a sharp leading edge with a flat surface on one side and a constant favorable-pressure-gradient surface on the other. Tests were made at Mach numbers of 1.61 and 2.01, over a Reynolds number per foot range from about 0.5×10^6 to approximately 9.5×10^6.

Transition at zero heat transfer was apparently strongly influenced by surface conditions. Transition Reynolds numbers for zero heat transfer ranged from 4×10^6 to 10×10^6 for the flat surface and from 4×10^6 to 16×10^6 for the favorable-pressure-gradient surface. Heating or cooling the model surface had little effect on transition when small and nearly undetectable surface roughness existed, but with surface roughness eliminated, surface cooling was quite effective in increasing transition Reynolds number. The first appearance of transition due to roughness behind single-element three-dimensional roughness and the lateral spread of turbulence as determined by the boundary-layer probe technique were in excellent agreement with results previously obtained on the identical configurations with a hot-wire technique. Installation of a sharp-edged plate or wedge so that the flat side of the wedge was alined with the stream had no effect on transition. Deflection of this surface in either the positive or negative direction generally resulted in large reductions in the values of transition Reynolds number.

INTRODUCTION

As part of a general investigation of transition in the Langley 4- by 4-foot supersonic pressure tunnel some tests were made to determine

the effects of surface cooling on boundary-layer transition on a parabolic body of revolution (ref. 1). These tests indicated that surface cooling had a strong effect on transition on a three-dimensional axisymmetric body. From theoretical considerations it can be deduced that this cooling phenomenon should be qualitatively the same on a two-dimensional body such as a wing, but quantitatively the effects may differ. Consequently, it appeared desirable to make similar studies of the effects of surface cooling on boundary-layer transition on a two-dimensional wing for comparison.

This two-dimensional transition study was made on a wing which spanned the tunnel. The wing had one flat surface, one approximately parabolic-arc surface, a sharp leading edge, and a thickness of 4.5 percent of the chord. Tests were made at Mach numbers of 1.61 and 2.01 over a Reynolds number per foot range from about 0.5×10^6 to 9.5×10^6. Maximum changes in average surface temperature due to cooling and heating of about -150° F and 150° F, respectively, were investigated, the values corresponding to incremental temperature ratios, in terms of the stagnation temperature, of -0.27 and 0.27. A limited number of tests were also made to determine the effects of discrete three-dimensional roughness on transition and the lateral spread of transition and to determine the effects of installing stub wings or wedges.

L 6 1 3

SYMBOLS

k	height of roughness particle
M	Mach number
p	local pressure within boundary layer indicated by total-pressure probe
p_∞	free-stream static pressure
p_t	stagnation pressure
R	Reynolds number based on flow outside boundary layer
R_{tr}	transition Reynolds number based on flow conditions outside boundary layer and distance from wing leading edge to transition location
T_t	stagnation temperature

ΔT	change in surface temperature due to cooling (average value except as noted)
u	local streamwise component of velocity in boundary layer
u_∞	local streamwise component of velocity just outside boundary layer
x	longitudinal distance from leading edge
y	lateral distance from tunnel center line, positive to the right
δ	angle between flat side of wedge and stream direction, positive when flat side becomes a compression surface

APPARATUS

Wind Tunnel

The investigation was conducted in the Langley 4- by 4-foot supersonic pressure tunnel, which is a rectangular, closed-throat, single-return wind tunnel with provisions for the control of the pressure, temperature, and humidity of the enclosed air. The test section width and height are approximately 54 inches. Flexible nozzle walls were adjusted to give the desired test-section Mach numbers of 1.61 and 2.01. During the tests, the dewpoint was kept below -20° F to insure negligible effects of water condensation in the supersonic nozzle.

Model

The model used in this investigation consisted of a rectangular two-dimensional wing which spanned the tunnel. Sketches of the wing are presented in figure 1 and a photograph of the wing is presented in figure 2. Details of the wedge installations are presented in figure 3. The span of the wing was $53\frac{1}{2}$ inches and the chord was 40 inches. One surface of the wing was flat and the other surface had an approximately parabolic surface which was designed by the method of characteristics to have a constant favorable pressure gradient at $M = 1.6$. The thickness-chord ratio was 4.5 percent and the leading-edge thickness generally varied between 0.004 and 0.006 inch. The model was constructed of $\frac{3}{4}$-inch boilerplate and the surfaces were polished. Owing to air holes incurred

in the rolling of the boilerplate, there were a large number of minute holes or pits of varying depth and size scattered over the surfaces.

The model was attached directly to the tunnel sidewall inserts at zero angle of attack. It was hollow and was vented to the outside of the tunnel at one end so that liquid carbon dioxide could be used to cool the model surfaces or superheated steam could be injected to heat them. A row of 18 iron-constantan thermocouples was installed on the outside surface of each model at about the tunnel center line to measure the temperature distributions.

TESTS

Techniques

Boundary-layer transition was determined by several methods. In the first phase of the tests, transition was determined by the use of rakes of total-pressure tubes in a manner similar to that described in reference 1. In the second phase of the tests, transition was identified by the use of a two-tube total pressure rake or probe which could be traversed across the wing (see fig. 1). These tubes had an external diameter of 0.050 inch. One tube lay directly on the surface (distance from surface to the tube center was 0.025 inch) and the other was placed with its center at a distance of 0.080 inch from the surface. The tubes were 26.8 inches rearward of the wing leading edge. Thus, for the range of conditions covered in this investigation, the surface tube indicated pressures within the inner part and the outer tube indicated pressures in the outer extremities of the laminar boundary layer. Transition was also determined in some of the phase II tests by means of a temperature-sensitive fluorescent lacquer. A discussion of the preparation of the lacquer and the methods of applying and interpreting the results can be found in reference 2.

The test procedure generally consisted of starting the tunnel at a low value of stagnation pressure and a corresponding small free-stream Reynolds number per foot and then gradually increasing the Reynolds number per foot in small increments to values greater than those required to identify transition from laminar to turbulent flow. At each increment in tunnel stagnation pressure or Reynolds number per foot, the tunnel conditions were stabilized and photographs were taken of the multiple-tube mercury manometer to which the rakes of the phase I tests were connected, or the total pressures indicated by the two-tube probe were visually read on a U-tube manometer and recorded. Simultaneously with the reading of the pressures, the fluorescent lacquer was visually inspected through small tunnel windows and its indications interpreted

in the phase II tests. Whenever it appeared desirable, the two-tube probe was also traversed across the wing and the spanwise variations in pressure were recorded.

For the tests with boundary-layer heating or cooling, the procedure was to set the tunnel stagnation pressure at the desired value and then to turn on the steam or liquid carbon dioxide until a prescribed maximum or minimum surface temperature was attained. At this point, the heating fluid or coolant was turned off and the model temperature returned to the zero-heat-transfer equilibrium condition. During this whole period, the distribution of surface temperature was continuously recorded on potentiometers. At time intervals determined by the rapidity of changes in the boundary-layer pressures, the boundary-layer total pressures and tunnel conditions were read and recorded. Spanwise traverses were made only near maximum cooling conditions with the coolant flowing continuously in order to insure the least possible change in model temperature with time.

Range of Conditions

The tests were made in two phases. In both phases tests were made at Mach numbers of 1.61 and 2.01 and over a Reynolds number per foot range from about 0.5×10^6 to 9.5×10^6. The phase I tests were terminated after a number of runs because surface cooling or heating had little or no apparent effect on boundary-layer transition and it was believed that surface roughness was influencing the results. In the time interval between the two test phases additional instrumentation was constructed to improve the boundary-layer survey technique and a temperature-sensitive lacquer was developed to aid in the determination of the model areas that might contain otherwise undetectable roughness.

In the phase I tests, transition was determined at about the 23.5- and 34.0-inch stations on both the flat and curved surfaces under adiabatic conditions and under conditions of heat transfer. For the tests with heat transfer, the model was cooled at a number of values of tunnel Reynolds number per foot above those for which transition had moved ahead of the pressure rake. Conversely, the model was heated at a number of values of Reynolds number per foot below those for which transition had moved to the rear of the rake. Maximum changes in average surface temperature of about -150° F and 150° F for surface cooling and heating, respectively, were employed, the temperature changes corresponding to $\Delta T / T_t$ values of -0.27 and 0.27. Some transition studies were made on the flat surface of the wing with the rake at the 23.5-inch station, the wing leading edge blunted by means of a strip of adhesive cellophane

tape, and balsa strips attached to the curved surface. These strips of balsa were 1/16, 1/8, and 1/4 inch in thickness.

In the phase II tests, a group of transition runs was made with the flat surface of the wing painted with temperature-sensitive lacquer to determine roughness spots and make possible their elimination. Then the phase I transition tests were repeated; however, the heat-transfer studies were limited to boundary-layer cooling and changes in leading-edge bluntness were limited to sharpening the leading edge to a thickness of about 0.002 inch. The pressure probe was always 26.8 inches from the leading edge. Tests were also made at $M = 1.61$ with 0.019-inch roughness (single 0.018-inch-diameter steel ball) and at $M = 2.01$ with 0.031-inch roughness (single 0.031-inch-diameter steel ball) located 8 inches from the wing leading edge. Finally, tests were made with wedges installed on the wing at three locations: wedge leading edge 3.5 inches ahead of, at, and 6 inches behind the wing leading edge. (See fig. 3.) For most of the tests with a wedge, the flat side of the wedge was at an angle between -3° and 3° relative to the stream flow direction.

RESULTS AND DISCUSSION

Phase I Tests

Zero heat transfer.- The results of the transition tests with zero heat transfer are summarized in figure 4. The vertical scale indicates transition Reynolds number; the horizontal scale differentiates the test Mach numbers and the rake locations from which the transition results were derived. Each data point represents a transition Reynolds number obtained in an individual test run. Inasmuch as the tunnel pressure was held constant while data were recorded, each transition Reynolds number can be considered as being time averaged at constant pressure because of the damping characteristics of the total-pressure rake system. No data are presented for the rearward rake location at $M = 1.61$ because the data were affected by disturbances originating at the wing-wall juncture. (See fig. 1.)

The data indicate two items of significance. First, there is a large amount of scatter in the transition Reynolds number. Many attempts were made to reduce this scatter by repolishing the model, with emphasis on the removal of any protuberances that could be found. These attempts were partially successful in that the transition Reynolds numbers were consistently higher when the model was carefully polished, but a considerable amount of scatter still remained. The conclusion to be derived from this trend is that transition was being affected by surface roughness. This conclusion is further supported by the transition results on

the constant favorable-pressure-gradient surface at $M = 2.01$. The lowest transition Reynolds numbers for both the forward and rearward rake locations occurred at about the same value of free-stream Reynolds number per foot, suggesting that transition occurred at the forward rake or ahead of it. This effect is typical of transition due to roughness.

The second item of significance is the large transition Reynolds numbers that were achieved. In particular, the maximum values of R_{tr} measured on the flat surface of the wing at $M = 1.61$ are as large as those measured on a 10° cone in the same facility at the same Mach number (ref. 3). At a constant free-stream Reynolds number per foot, the boundary layer on the flat plate is thicker than that on a cone at equal distances from the nose or leading edge by a factor of $\sqrt{3}$. If it is assumed that transition occurs at the same Reynolds number (based on the boundary-layer displacement or momentum thickness) on both models, the transition Reynolds number for the flat plate, based on the distance from leading edge to transition, will be only one-third that of the cone, based on the similar distance. The explanation may lie in the different rates of amplification of the initial pressure disturbances for the cone and flat plate, as discussed in reference 4.

Another possible source of the high values of R_{tr} was, at first, believed to be the relative bluntness of the leading edge. However, subsequent tests indicated that this was probably not a factor. Blunting the leading edge with cellophane tape (with downstream edges of the tape either faired or not faired) reduced the transition Reynolds number to about 4×10^6, and further blunting with balsa strips on the curved surface had even more drastic effects. Sharpening the leading edge from 0.004 inch to 0.002 inch had little or no effect on R_{tr}.

With heat transfer.- No data are presented for the phase I tests with heat transfer because (except for very small changes on the constant favorable-pressure-gradient surface at large heating rates) no effects of heat transfer, either heating or cooling, could be detected on transition for surface heating or cooling incremental temperature ratios as large as ± 0.27. This result was contrary to expectations; hence, considerable effort was expended in trying to eliminate any possible sources of surface roughness, as it was believed that small protuberances were responsible for the loss of the expected heat-transfer effect. The effort was unsuccessful, apparently because of the rather small protuberances which had to be located on a relatively large surface area.

Phase II Tests

Smooth wing.- The first tests in the phase II series were made at $M = 1.61$ with the flat surface of the wing painted with temperature-sensitive lacquer. As the tunnel stagnation pressure was increased (increasing the Reynolds number per foot) the fluorescent paint indicated an increasing number of scattered turbulent-flow wedges. The tunnel was shut down and the protuberances causing the premature transition were eliminated. This procedure was repeated a few times until there was, with one exception, no evidence of transition due to roughness up to a Reynolds number per foot of about 5.5×10^6. Beyond this value, transition due to the roughness of the paint appeared almost simultaneously over the whole wing in areas not already turbulent from other sources of boundary-layer transition. Inasmuch as the maximum Reynolds number $\left(5.5 \times 10^6 \text{ per foot}\right)$ for which the fluorescent lacquer had any usefulness was lower than the Reynolds number for which transition had been obtained on the parabolic surface in the phase I tests without heat transfer, it was decided to forego any further testing on that surface.

With the effects of roughness essentially eliminated, it was possible to follow the development of the transition pattern on the smooth wing. First, even at the lowest values of Reynolds number per foot, a wedge of turbulent flow existed about 8 inches to the left of the tunnel center line. This turbulent flow was caused by screw holes which had been drilled in order to install wedges for later tests, even though the holes were filled with dental plaster and faired. As the Reynolds number per foot was increased from the lowest values, all the wing area to the rear of the pressure disturbances from the wing-wall juncture (which propagated along lines having angles close to those of the Mach lines) was rapidly covered by turbulent flow. With further increases in tunnel stagnation pressure, the transition front began to move toward the wing leading edge from the apex of the V formed by the Mach lines until it was lost owing to the aforementioned transition due to paint roughness. These transition indications were corroborated at the 26.8-inch station of the wing by pressure changes determined with the two-tube probe, and they were also in agreement with the average results of the phase I tests.

The results of the tests with boundary-layer cooling, in which the same temperature-sensitive lacquer and total pressure probe technique were used, are presented in figure 5. It should be noted that the probe location was always used as the reference station for determining transition. The data are compared with results obtained on a three-dimensional body of revolution, the RM-10 (ref. 1). Inasmuch as the reference transition Reynolds numbers with zero heat transfer are different in each case, the data have been plotted in terms of the transition Reynolds number ratio $R_{tr} / \left(R_{tr}\right)_{\Delta T=0}$, where the reference zero-heat-transfer transition

Reynolds number is that for the corresponding model. The temperature ratio $\Delta T/T_t$ is the average value of cooling from the model leading edge to the transition point. A plot of a few typical temperature distributions for the wing is presented in figure 6. It was impossible to cool the leading edge because the edge was solid for the first 4 inches or so. This lack of cooling is probably of no significance for the range of Reynolds numbers per foot involved in these tests and for the constant transition location.

The results of figure 5 indicate that there is a favorable effect of boundary-layer cooling. From these data and from the previous discussion about eliminating roughness effects, it appears that the lack of any heat-transfer effects in the phase I tests must be ascribed to surface roughness which could not be readily detected. Whether the cooling effects on transition are stronger in the two-dimensional (wing) case than in the three-dimensional (RM-10 body) case may be open to question, as the scatter in the present tests is rather large and changes in a few of the more strategic points could easily alter the slope of the curve.

Similar tests at $M = 2.01$ again indicated a favorable effect of cooling on transition, but insufficient data were obtained to establish any curve.

Wing with roughness.- A single-element three-dimensional roughness particle (steel sphere) was cemented to the wing at $x = 8$ inches and the effect on transition at the probe location is shown in figure 7 for $M = 1.61$. The probe was directly in line with the roughness element. The ordinate is the total-pressure coefficient $\frac{p - p_\infty}{p_t}$ indicated by the total-pressure tubes as the free-stream Reynolds number per foot was increased. The experimental values are indicated by the symbols; the theoretical laminar values computed by the method of reference 5 are represented by the dashed lines. The dotted horizontal lines denote the theoretical total-pressure-ratio coefficient just outside the laminar boundary layer.

Examination of both the (a) and (b) parts of figure 7 indicates that, as the free-stream Reynolds number per foot was increased from the lowest values, the total pressures indicated by the probes also increased because of the thinning of the laminar boundary layer. The quantitative agreement with theory was not always very good, but the agreement of the trends was good. As the Reynolds number per foot was further increased in the case of the smooth wing, the outer tube left the boundary layer and ceased to show any changes in pressure, whereas the surface tube still indicated a rising pressure in agreement with theory. At a Reynolds

number per foot of about 2.4×10^6, transition occurred, the boundary layer thickened, and the shape of the velocity profile changed. As a consequence, the outer tube was again plunged into the boundary layer and showed a decreasing total pressure. The surface tube was more strongly affected by the increase in velocity in the inner part of the boundary layer than by the increase in thickness and, hence, showed an increase in pressure at transition. As the Reynolds number per foot was further increased, the boundary layer became fully turbulent at the measuring station, and increased in thickness as a result of the forward movement of transition; then even the surface tube began to show a decreasing total pressure. For the case of transition behind the roughness (fig. 7(b)), transition occurred at a Reynolds number of about 1.45×10^6 per foot, before the outer tube moved out of the boundary layer. It should also be noted that after transition neither the outer nor the surface tubes showed any changes in total pressure with changes in Reynolds number per foot. This trend indicates that the boundary-layer thickness was not changing appreciably and implies that transition had moved up to the roughness element quickly and remained there. It should be noted that this indication has been contradicted by other results (ref. 6) and needs further investigation.

The value of Reynolds number per foot for which transition occurred at the probe location was in excellent agreement with the indications of a hot-wire technique (ref. 7) on the identical configuration. Similar results (not shown) were obtained at $M = 2.01$.

At this point, it is desirable to go into more detail about the interpretation of the changes in boundary-layer total pressures. This is done with the aid of figure 8, which shows typical laminar and turbulent velocity profiles and a sketch of a total-pressure tube at three vertical heights. Position 1 corresponds closely to the usual relative location of the outer tube. In general, the tube is in the outer region of the laminar boundary layer. If the Reynolds number per foot is increased and there is no transition, then the tube may emerge from the boundary layer and indicate a constant pressure coefficient with further increase in tunnel pressure. If transition occurs, the boundary layer thickens and the tube moves into a region of lower velocity and lower total pressure. The relative location of the surface tube, on the other hand, generally lies in the region indicated by positions 2 and 3. If transition occurs at high values of the Reynolds number per foot the surface tube is usually at a location slightly above position 2 and the tube may indicate a decreasing pressure. At slightly lower values of transition Reynolds number per foot the tube will be close to position 2 and may show no immediate change. If transition occurs at very low values of the Reynolds number per foot, the surface tube may be in a location corresponding to position 3 or lower, and the tube will indicate a rising total pressure. The sharper rise in pressure indicated by the

surface tube for transition behind the roughness at a Reynolds number per foot near 1.5×10^6, as compared with the more gentle rise experienced on the smooth wing at a Reynolds number per foot near 2.4×10^6, illustrates these trends. (See fig. 7.)

The explanation for the quantitative disagreement between the theoretical and experimental laminar pressures for the outer tube at low Reynolds number is not known, but it may be due, in some cases, to slight inadvertent changes in tube height relative to the surface from the value measured and used for the theoretical calculations. In any event, because of the emergence of the outer tube from the boundary layer and the dependence of the surface tube pressures on the Reynolds number per foot values for transition, transition is best determined by a simultaneous study of the pressure indications of both tubes.

The spanwise distribution of boundary-layer probe pressures for both the smooth wing and the wing with the roughness element is presented in figures 9(a) and 10. At $M = 1.61$, the comparison is at constant Reynolds number per foot and the pressures outside the turbulent wedge are in very good agreement. At $M = 2.01$, the pressures for the smooth wing are shown for a somewhat higher Reynolds number per foot than those for the wing with roughness. The low values of total pressure indicated by the outer tube at stations near $y = -8$ inches are due to the aforementioned effects on transition of the wedge mounting screw holes. Within the wedge of turbulent boundary layer, the pressures indicate that the boundary layer is thickest directly behind the roughness and decreases in thickness gradually to the smooth-wing value at the outer edge.

The effect of increasing Reynolds number per foot on the spanwise pressures behind the roughness was negligible within the wedge of turbulent boundary layer except near the wing surface toward the outer extremities of this region (fig. 9(b)). Boundary-layer cooling also had but slight effect (fig. 9(c)).

A comparison of the lateral spread of turbulence as determined by the total-pressure probe technique of this investigation and the results obtained on the identical configuration by a hot-wire technique (ref. 7) is presented in figure 11. Inasmuch as the effects of charges in Reynolds number have been shown to be negligible, the data from the two investigations can be considered to be in excellent agreement. The turbulent-wedge half-angles for the two Mach numbers of 1.61 and 2.01 are about 9.7° and 6.9°, respectively. Because sufficient data were not obtained at $M = 2.01$ to indicate that transition was probably at the roughness at the Reynolds numbers under discussion, it is not known whether the relatively large decrease in angle of lateral spread of turbulence is a true representation of the favorable effects of increasing Mach number.

Effect of shock impingement.- The effects of shock impingement on boundary-layer transition are presented in figure 12 for $M = 1.61$ and figure 13 for $M = 2.01$. These plots are similar to the first ones (fig. 7) discussed under the effects of roughness. For most of the results presented the probe was located at $y = 2$ inches, although in a few instances the probe was also located at $y = 0$. Both of these stations were well outside the area influenced by the wake from the wedge. The estimated transition points on the curves for the various wedge angles are indicated by short vertical lines. An arrow attached to these lines indicates that the transition point cannot be located, but is at a lower value of Reynolds number per foot than that indicated by the line. Ticks on the symbols specify that the data were obtained with decreasing tunnel pressure. There was no hysteresis in the results. The partially filled symbols in figure 12(a) indicate an interrupted run.

L 6 1 3

Examination of figures 12 and 13 shows that installing a wedge at 0° had little or no effect on transition when compared with smooth-wing results (fig. 7(a)). Increasing the wedge angle in the positive direction and generating a shock on the wing caused a sharp reduction in transition Reynolds numbers. Similarly, decreasing the wedge angle to negative angles and producing an expansion region across the wing surface decreased the transition Reynolds numbers, except for the most rearward wedge location at $\delta = -3^\circ$ and $M = 2.01$.

The transition results of figures 12 and 13 are summarized in figure 14, where the transition Reynolds number R_{tr} is plotted as a function of the wedge angle δ. At $M = 1.61$, the transition Reynolds numbers were generally higher for the wing with the wedge at 0° than for the smooth wing. This can probably be explained by the relatively large scatter inherent in the data. Had more phase II tests been made on the smooth wing, some higher smooth-wing transition Reynolds numbers would probably have been attained. At both Mach numbers, either increasing or decreasing the wedge angle caused a sharp reduction in R_{tr} except for the most rearward wedge location at $\delta = -3^\circ$ and $M = 2.01$. This reduction in R_{tr} at negative values of δ is somewhat surprising, inasmuch as a favorable pressure gradient should be created on the wing in the region of interest. Because the boundary layer tends to flow in the direction of decreasing static pressure, whereas the outer flow follows the potential, there will be a difference in the boundary-layer and potential-flow directions. This difference in flow direction causes a tendency for the boundary layer to roll up and presumably could accelerate transition. This roll-up tendency exists for both the compression (positive δ) and expansion (negative δ) cases. The data of figure 13 indicate that a relatively small wedge deflection from 0° (of 0.6° or perhaps less) had an adverse effect on transition.

In order to obtain information that might be helpful in determining the origin of the wedge effect on transition, a few spanwise surveys were made. Some of these are presented in figures 15 to 20. The figures are similar to the spanwise surveys presented for the single-element roughness data, with the additional identification of several items of interest. The wedge wake is shown to occur in the region near $y = -8$ inches, which was affected by early transition because of the screw holes, as discussed previously, and hence the wake is difficult to identify. The estimated locations of the trailing-edge expansion (wedge had a blunt trailing-edge) and the limit of transverse contamination (assuming a 10° half-wedge angle originating at the wedge leading edge) are also presented. Far to the right, in the area of $y = 7$ to 9 inches approximately, is indicated the estimated location of the leading-edge shock or expansion wave.

The results of the spanwise surveys indicate that at $M = 1.61$ the installation of the wedge at 0° had little or no effect (fig. 15(a)). Installation of a wedge at $\delta = -3^\circ$ in the rearward location at this Mach number caused a decreasing transition Reynolds number (decreasing total pressure of outer tube) as the wedge was approached. Away from the wedge and near the leading-edge wave location there was little effect. The decrease in pressures outboard of the wave location for both the smooth wing and the wing with the wedge installed is due to early transition caused by tunnel sidewall effects and surface roughness effects and should be discounted. The effect of deflecting the wedge from 0° to 3° (fig. 16(a)) shows trends similar to those just discussed for the installation of the wedge, as is to be expected. The effects of increasing Reynolds number as illustrated by the results of figure 16(b) are somewhat confusing. At a Reynolds number per foot of 1.11×10^6 the data of figure 12(c) indicate that the boundary layer is laminar at $y = 0$ although the pressures do appear to be somewhat low when compared with the theoretical predictions. The data of figure 16(c) for a Reynolds number per foot of 1.1×10^6, on the other hand, indicate a decreasing pressure in the region of the outer tube as the wedge is approached, which is an indication of transition. At a Reynolds number per foot of 2.80×10^6, transition has definitely occurred at this spanwise station. It therefore appears that the boundary layer was abnormally thick or in partial transition at the lower Reynolds number and decreased in thickness at an abnormal rate, or that the boundary layer became more laminar as the Reynolds number per foot was increased and before transition actually occurred in the region close to the wedge.

At $M = 2.01$ the installation of wedges at either -3° or 3° in the middle wedge location had the same effect on transition as at $M = 1.61$ (figs. 17(a) and 17(b)). The effect on transition appears to be somewhat stronger for the positive deflection. It should be noted at this

point that there was no shock detachment from the wedge leading edge for either $M = 1.61$ or $M = 2.01$ with the wedge deflections under consideration. At a Reynolds number per foot of 3.45×10^6, the flow was already turbulent at the probe location on the smooth wing. Installation of the wedges at $\delta = -3^\circ$ and 3° appears to create a tendency toward a decreased transition Reynolds number close to the wedge even in this case (figs. 18(a) and 18(b)).

Some effects of Reynolds number on transition at $M = 2.01$ with wedges installed are shown in figure 19. For the negative wedge deflection case, where installation of the wedge had little effect on transition in the spanwise region near the leading-edge expansion wave, increasing the Reynolds number caused transition to move forward in this region but had little effect in the area next to the wedge. For the positive wedge deflection, there was no effect due to Reynolds number.

The effect of varying the wedge angle at constant Reynolds number is presented in figure 20. At a Reynolds number per foot of 1.48×10^6, changing the wedge angle from -3° to 3° resulted in reduced transition Reynolds numbers near the wedge leading-edge-shock or expansion-wave location. At the high test Reynolds number, there were no significant effects with the exception that transition may be in a more forward location for the $\delta = -3^\circ$ configuration.

CONCLUSIONS

An exploratory investigation has been made to determine the effects of single-element surface roughness, boundary-layer cooling, and shock impingement on transition on a two-dimensional wing at Mach numbers of 1.61 and 2.01. Analysis of the results of the tests indicates the following conclusions:

1. Transition at zero heat transfer was apparently strongly influenced by surface conditions. Transition Reynolds numbers for zero heat transfer ranged from 4×10^6 to 10×10^6 for the flat surface and from 4×10^6 to 16×10^6 for the approximately parabolic surface with the favorable pressure gradient.

2. Heating or cooling the model surface had little effect on boundary-layer transition when small and nearly undetectable surface roughness existed, but with surface roughness eliminated, surface cooling was quite effective in increasing the transition Reynolds number.

3. The first appearance of transition due to roughness behind a single-element three-dimensional roughness and the lateral spread of turbulence as determined by the boundary-layer probe technique were in excellent agreement with results previously obtained on the identical configurations with a hot-wire technique.

4. Installation of a wedge so that the flat side of the wedge was alined with the stream had no effect on transition. Deflection of this surface in either the negative or positive direction generally resulted in large reductions in the values of transition Reynolds number.

5. At low free-stream Reynolds numbers per foot, where the effects of the wedge on transition were strong, the largest decreases in transition Reynolds number occurred close to the wedge and the smallest effects were felt outward in the neighborhood of the wedge leading-edge shock or expansion wave.

Langley Research Center,
National Aeronautics and Space Administration,
Langley Field, Va., April 6, 1960.

REFERENCES

1. Czarnecki, K. R., and Sinclair, Archibald R.: An Investigation of the Effects of Heat Transfer on Boundary-Layer Transition on a Parabolic Body of Revolution (NACA RM-10) at a Mach Number of 1.61. NACA Rep. 1240, 1955. (Supersedes NACA TN's 3165 and 3166.)

2. Loving, Donald L., and Katzoff, S.: The Fluorescent-Oil Film Method and Other Techniques for Boundary-Layer Flow Visualization. NASA MEMO 3-17-59L, 1959.

3. Sinclair, Archibald R., and Czarnecki, K. R.: Investigation of Boundary-Layer Transition on 10° Cone in Langley 4- by 4-Foot Supersonic Pressure Tunnel at Mach Numbers of 1.41, 1.61, and 2.01. NACA TN 3648, 1956.

4. Tetervin, Neal: A Discussion of Cone and Flat-Plate Reynolds Numbers for Equal Ratios of the Laminar Shear to the Shear Caused by Small Velocity Fluctuations in a Laminar Boundary Layer. NACA TN 4078, 1957.

5. Chapman, Dean R., and Rubesin, Morris W.: Temperature and Velocity Profiles in the Compressible Laminar Boundary Layer With Arbitrary Distribution of Surface Temperature. Jour. Aero. Sci., vol. 16, no. 9, Sept. 1949, pp. 547-565.

6. Jackson, Mary W., and Czarnecki, K. R.: Investigation by Schlieren Technique of Methods of Fixing Fully Turbulent Flow on Models at Supersonic Speeds. NASA TN D-242, 1960.

7. Braslow, Albert L., Knox, Eugene C., and Horton, Elmer A.: Effect of Distributed Three-Dimensional Roughness and Surface Cooling on Boundary-Layer Transition and Lateral Spread of Turbulence at Supersonic Speeds. NASA TN D-53, 1959. (Supersedes NACA RM L58A17.)

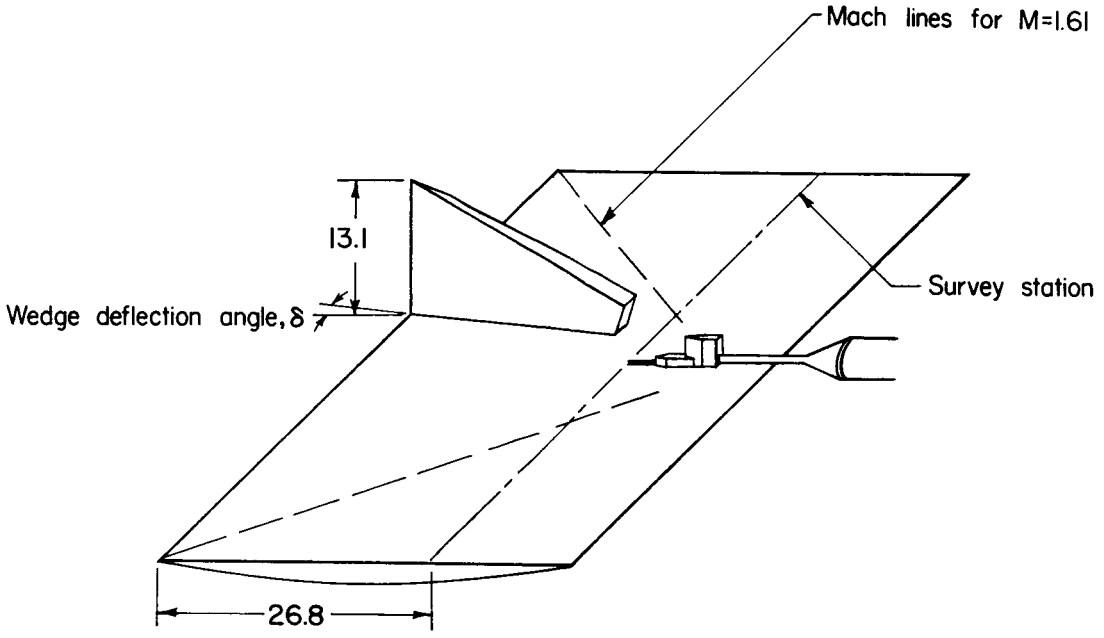

(a) Wedge configuration.

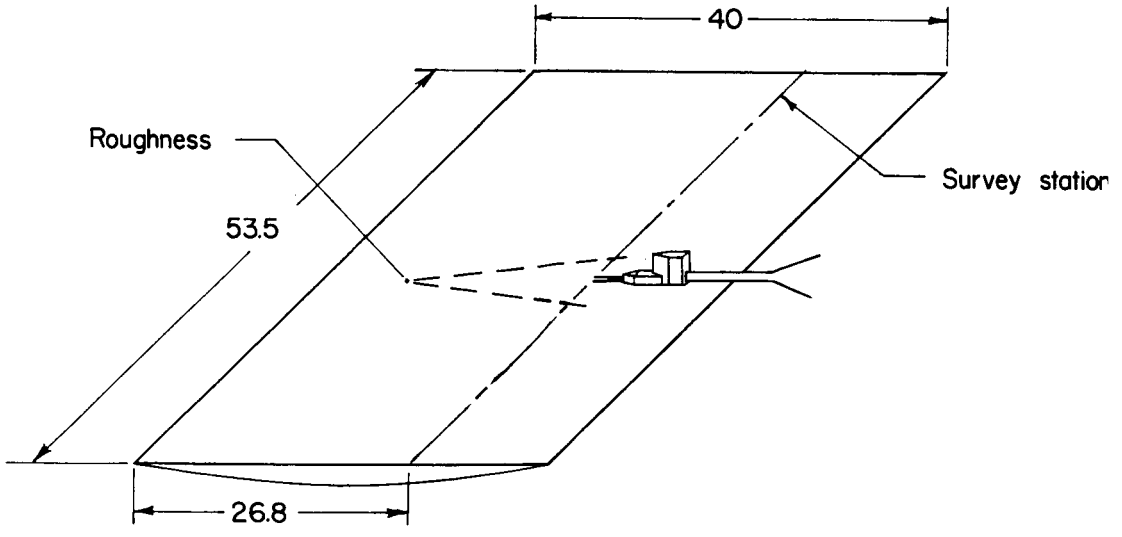

(b) Roughness configuration.

Figure 1.- Sketch of model. All dimensions are in inches.

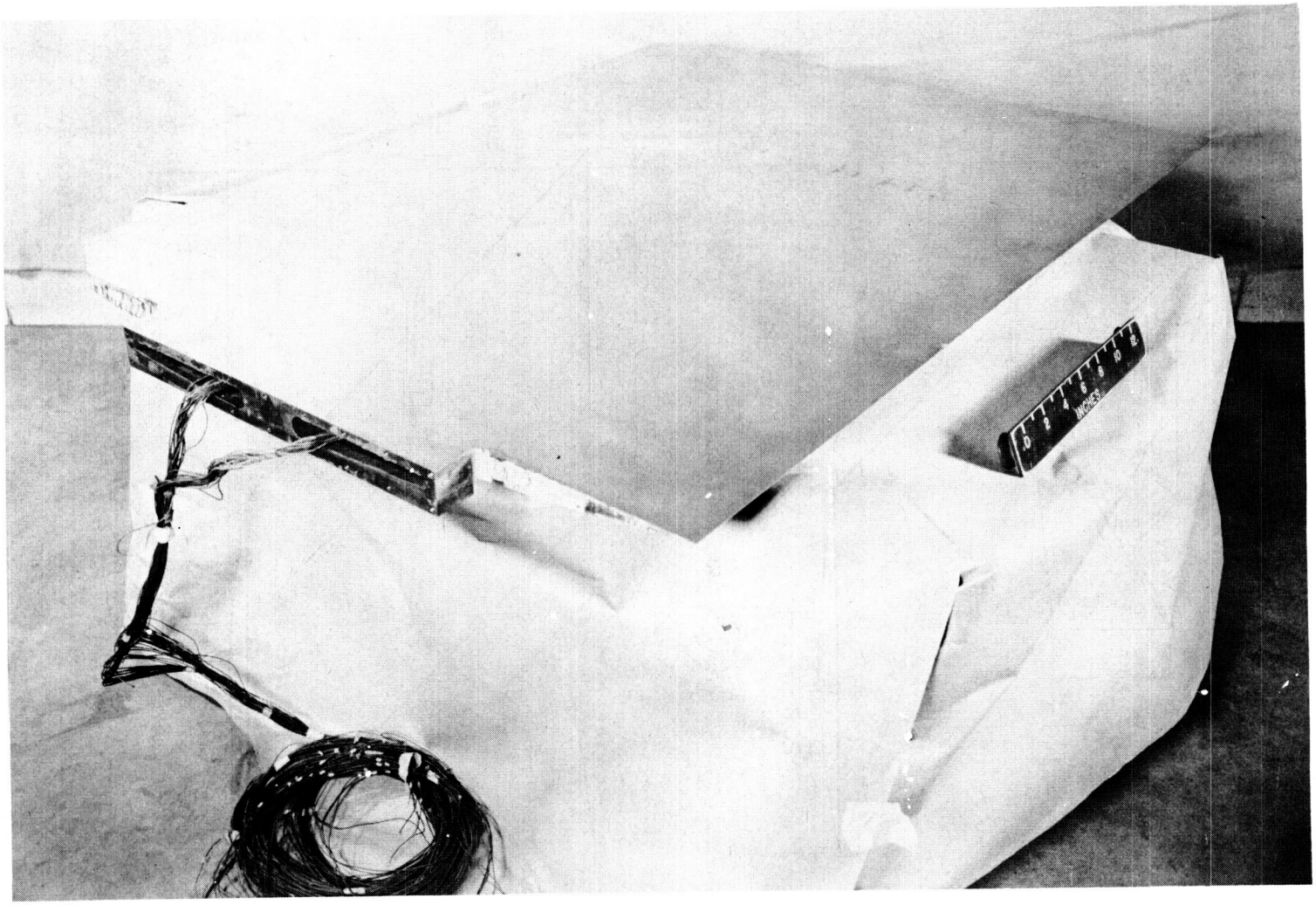

Figure 2.- Photograph of wing. L-59-1463

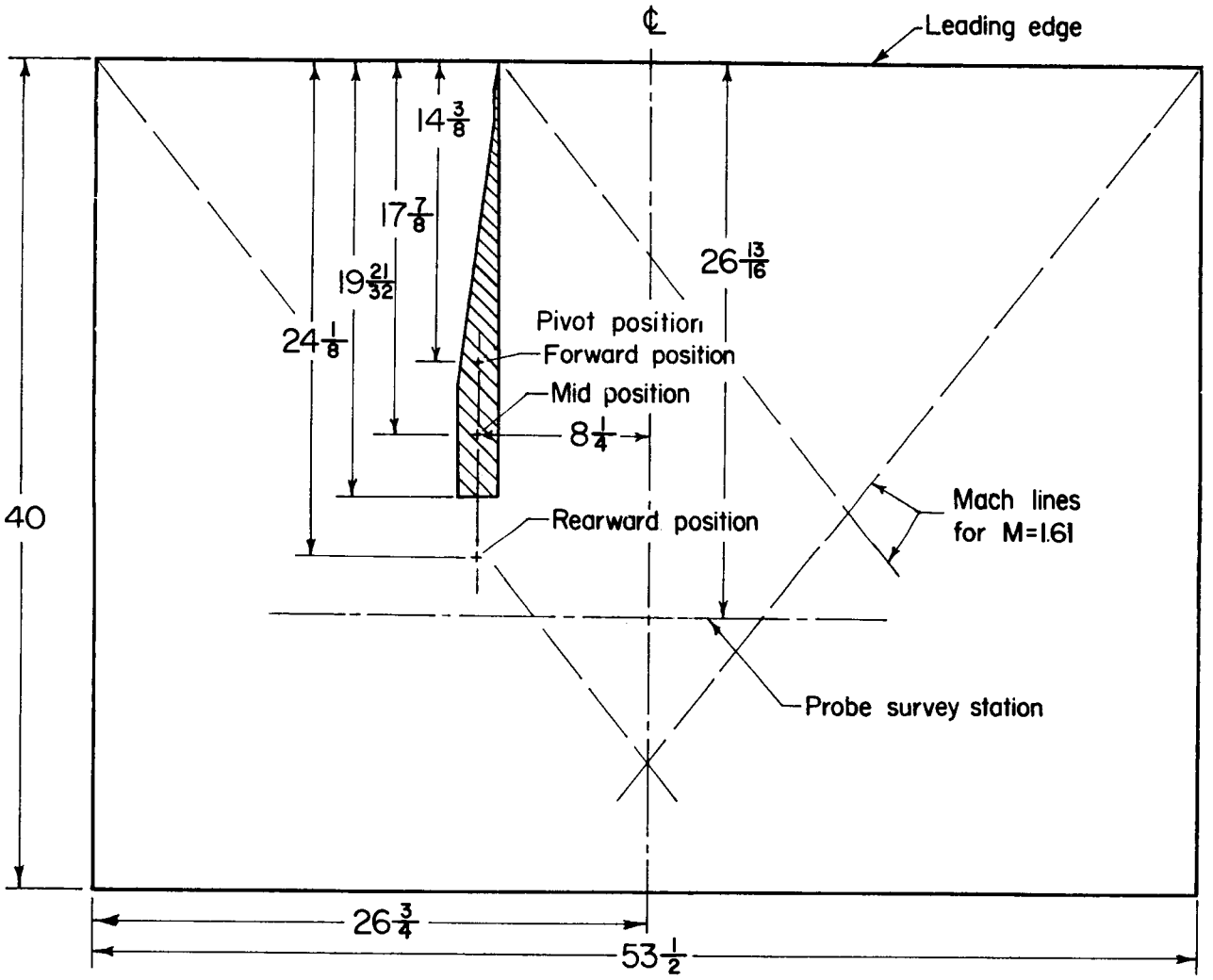

Figure 3.- Details of wedge installations. All dimensions are in inches.

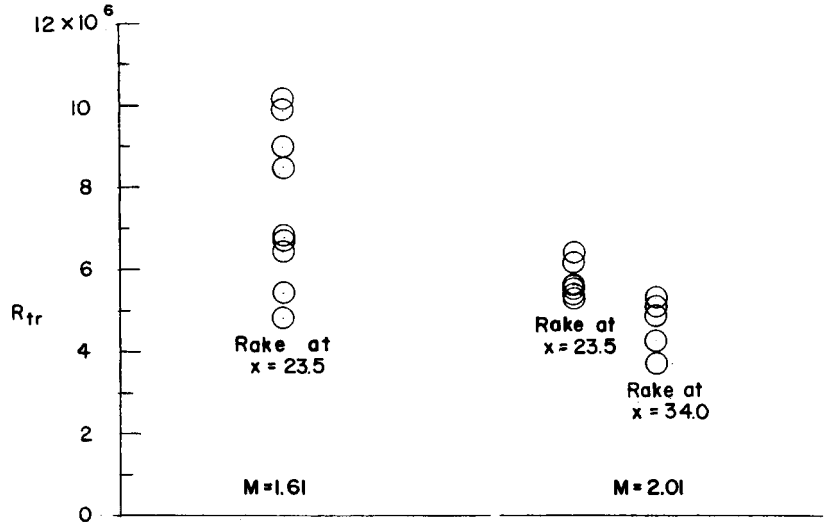

(a) Flat surface.

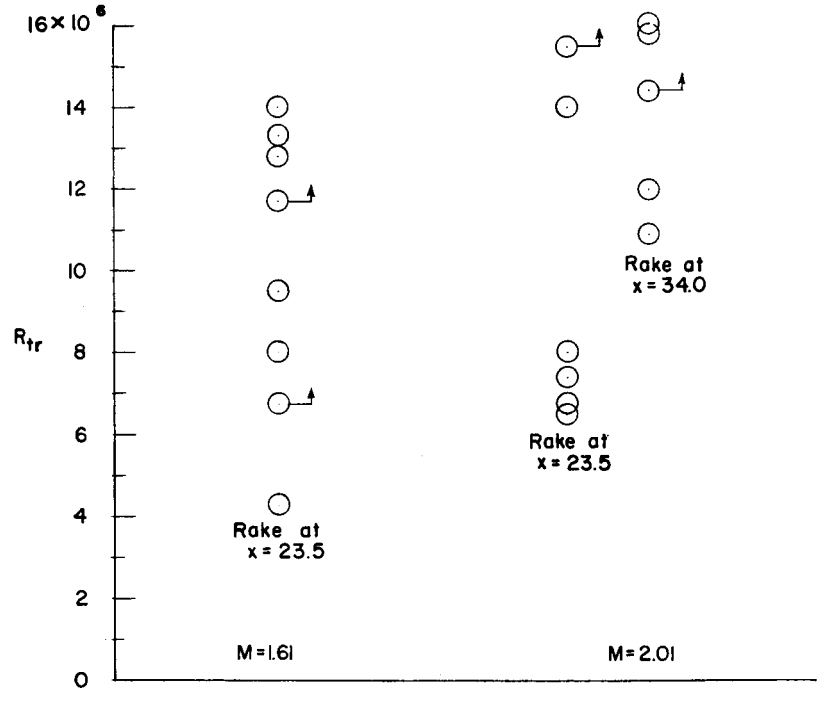

(b) Constant favorable-pressure-gradient surface.

Figure 4.- Summary of phase I transition results. Zero heat transfer. Arrows indicate that actual values are unknown but are larger than those indicated. Station x is in inches.

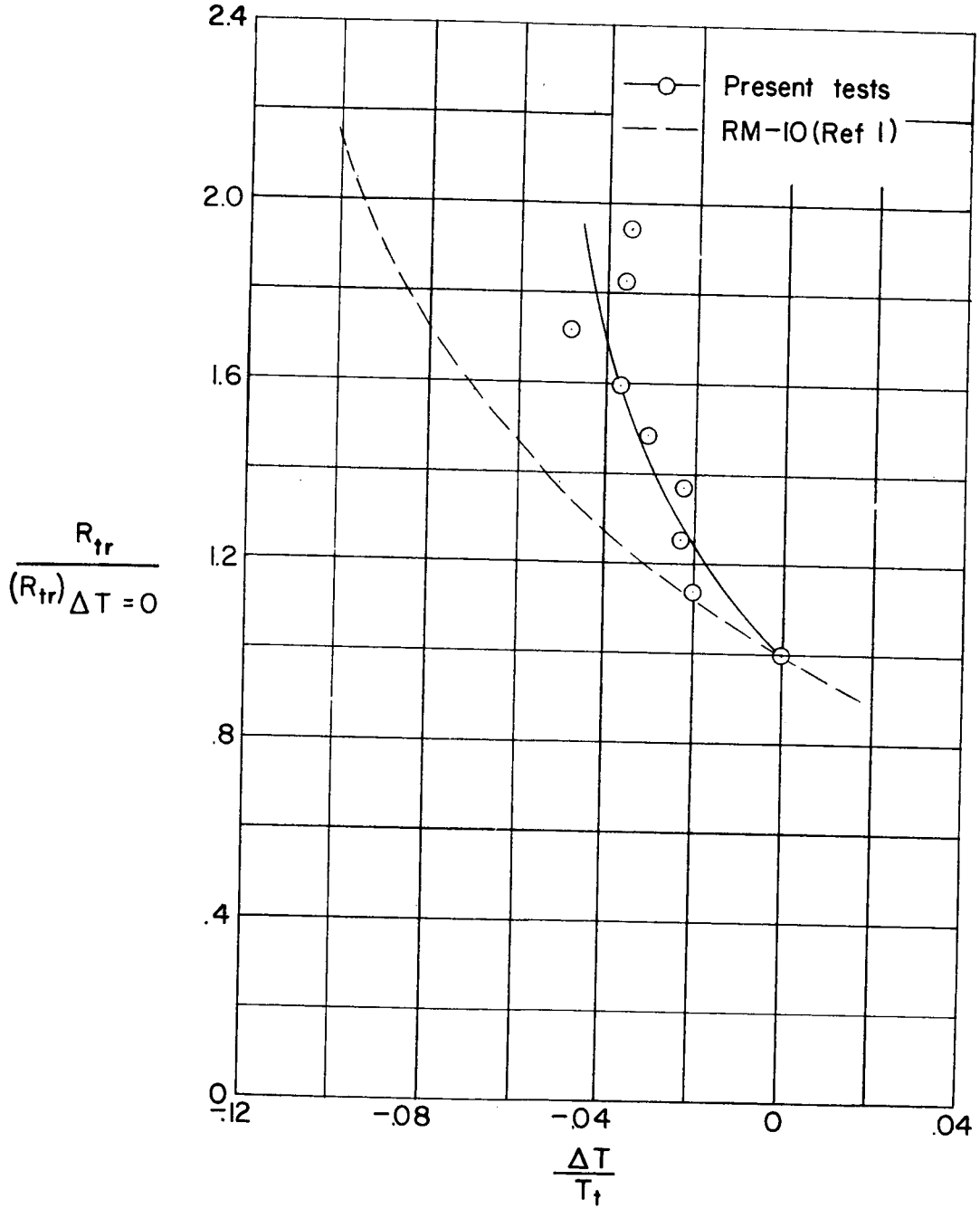

Figure 5.- Effect of surface cooling on boundary-layer transition Reynolds number ratio. Transition location is at boundary-layer probe. M = 1.61; $(R_{tr})_{\Delta T=0} = 5.35 \times 10^6$ for present tests.

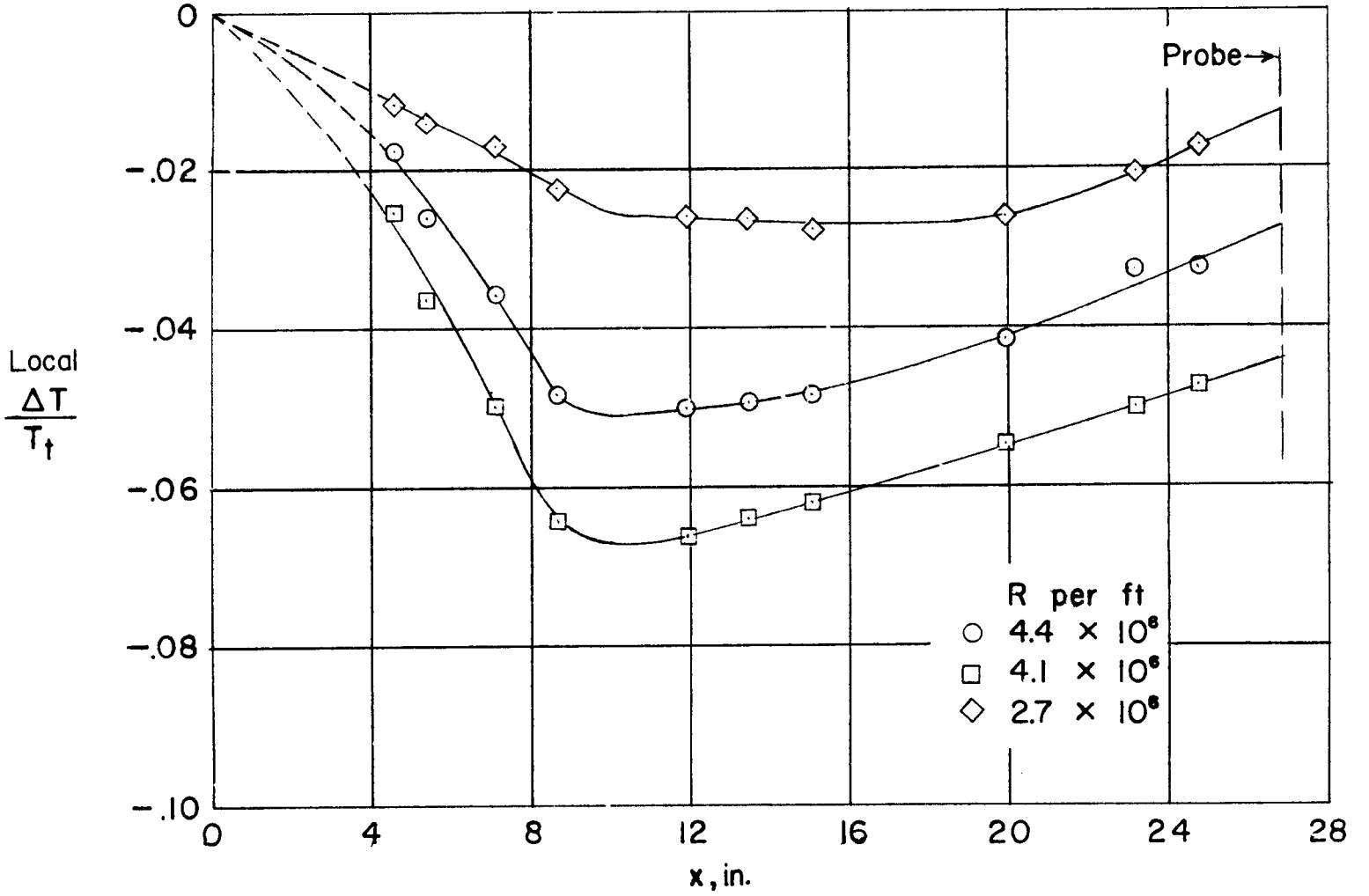

Figure 6.- Typical temperature distributions with surface cooling when transition occurred at boundary-layer probe location. M = 1.61.

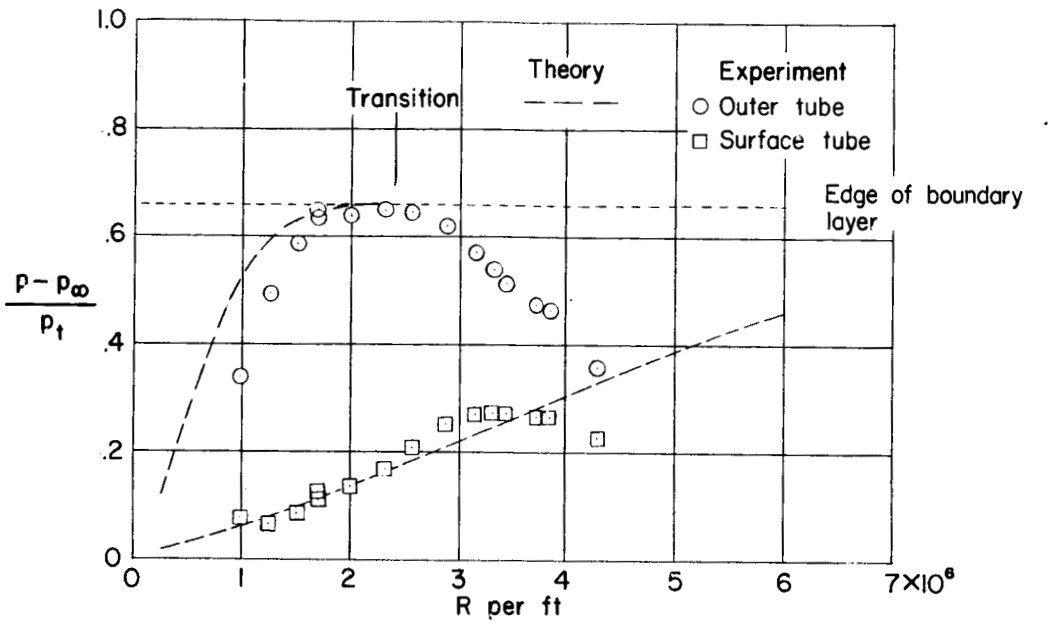

(a) Smooth wing.

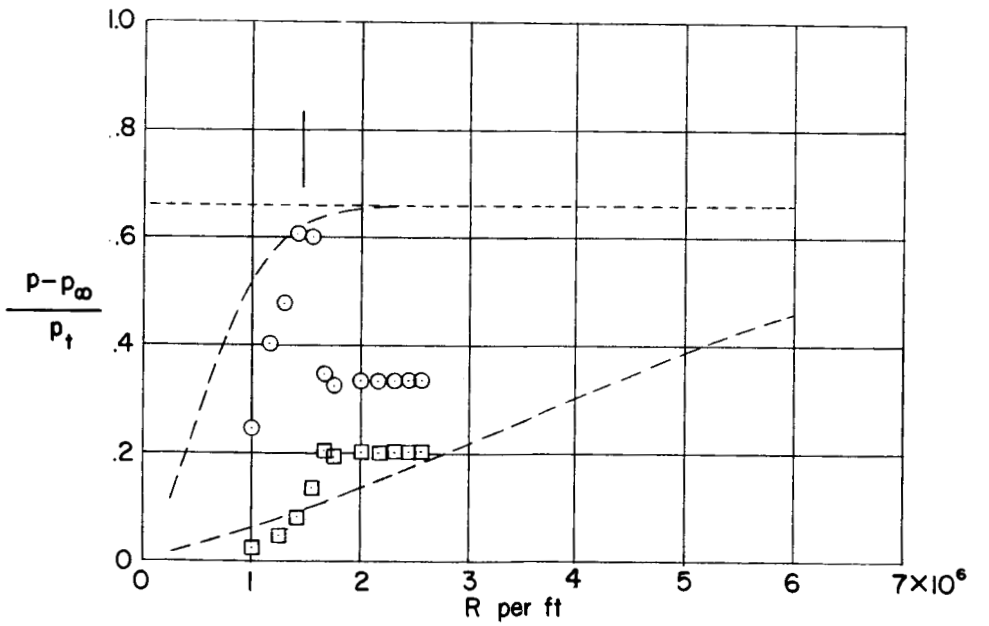

(b) k = 0.019 inch at x = 8 inches.

Figure 7.- Effect of single-element three-dimensional roughness on boundary-layer probe pressures. M = 1.61; y = 0.

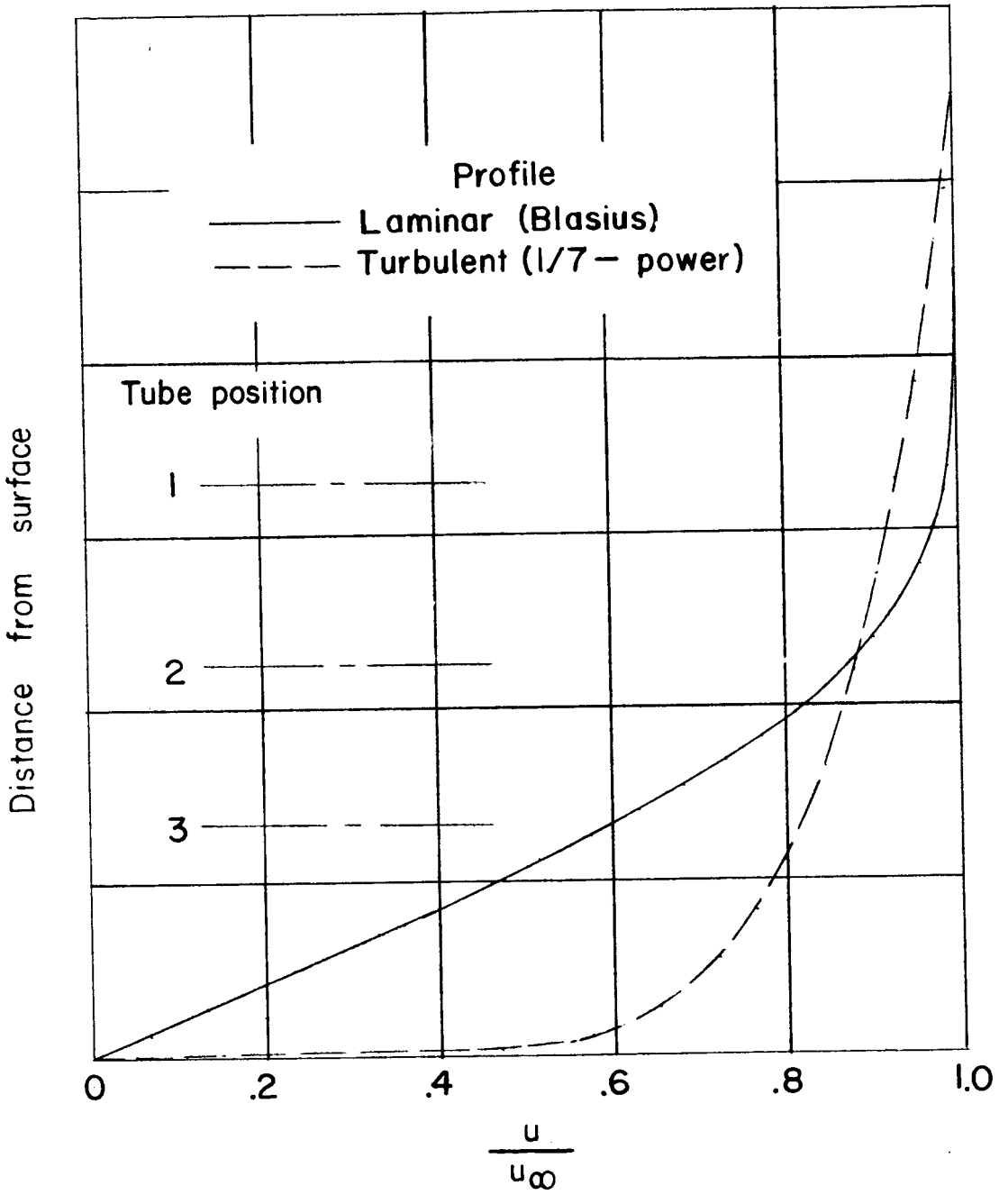

Figure 8.- Effects of changes in boundary-layer profiles and thickness on trends in boundary-layer probe response.

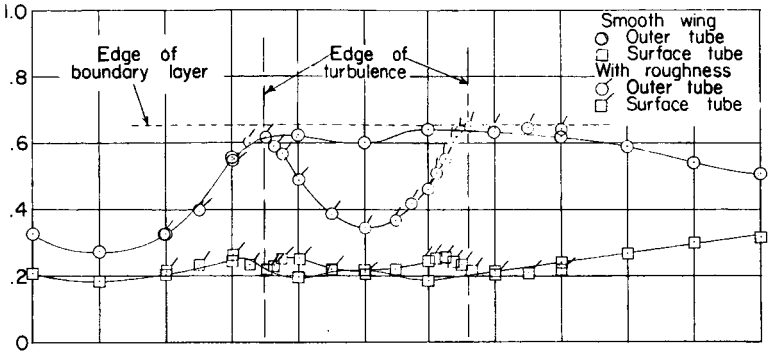

(a) Effect of installing roughness; Reynolds number per foot = 2.57×10^6.

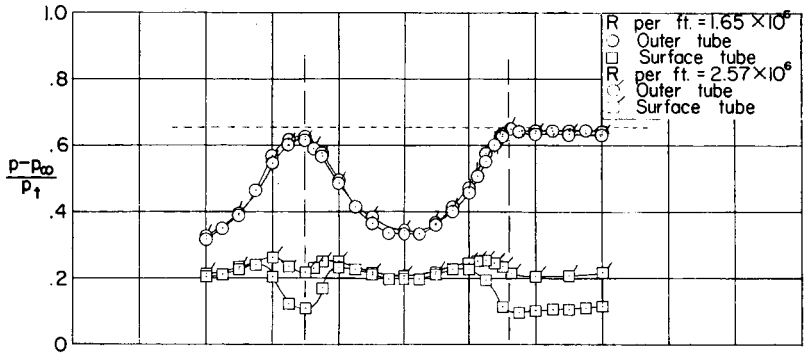

(b) Effect of Reynolds number per foot.

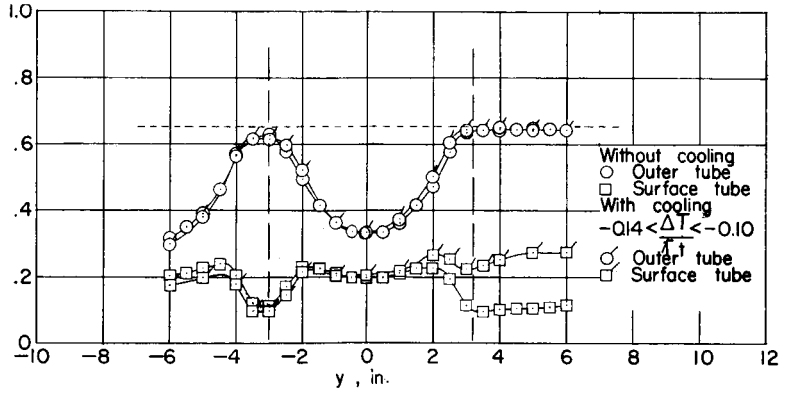

(c) Effect of boundary-layer cooling; Reynolds number per foot = 1.65×10^6.

Figure 9.- Effect of Reynolds number per foot and boundary-layer cooling on the lateral spread of turbulence. M = 1.61; k = 0.019 inch at x = 8 inches and y = 0 inch.

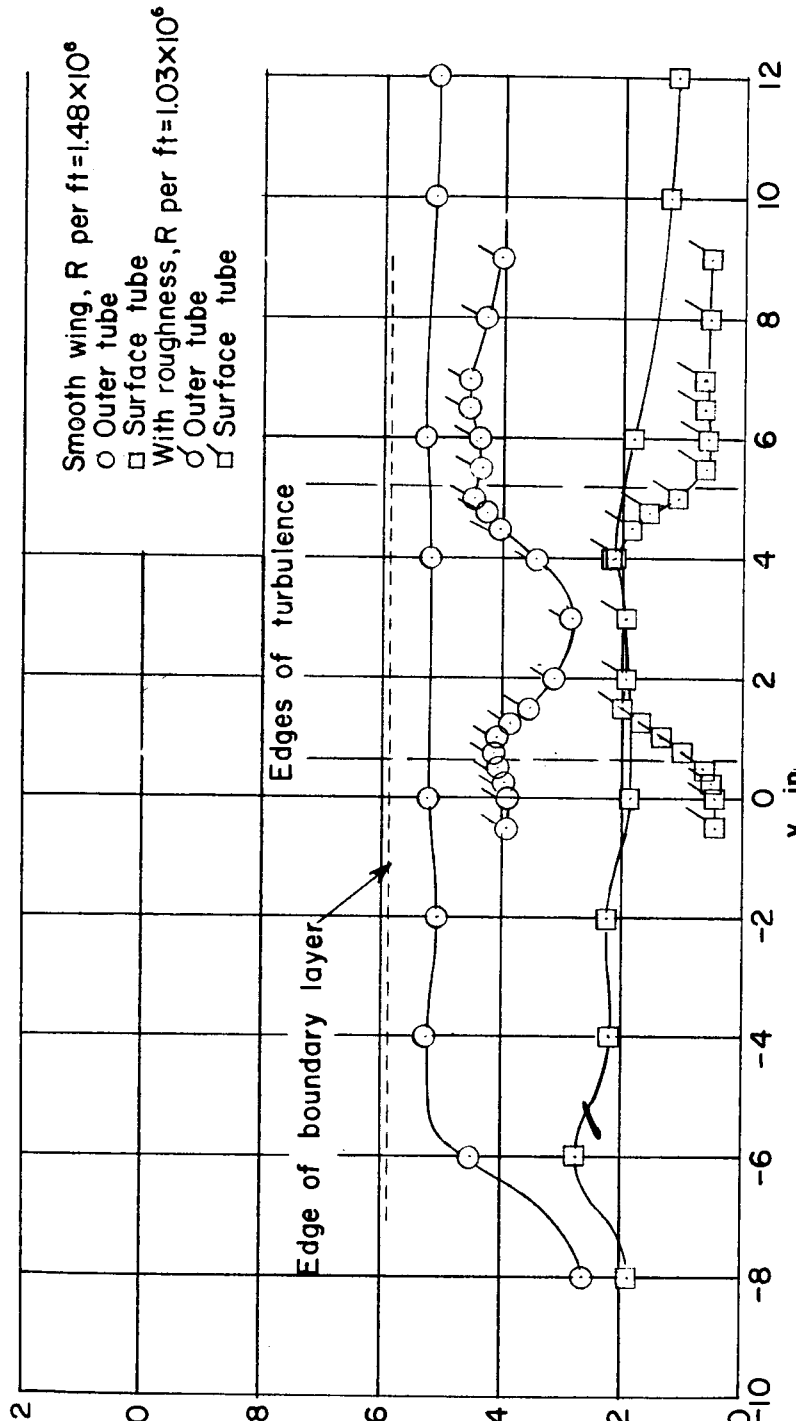

Figure 10.- Lateral spread of turbulence behind single-element three-dimensional roughness. M = 2.01; k = 0.031 inch at x = 8 inches and y = 3 inches.

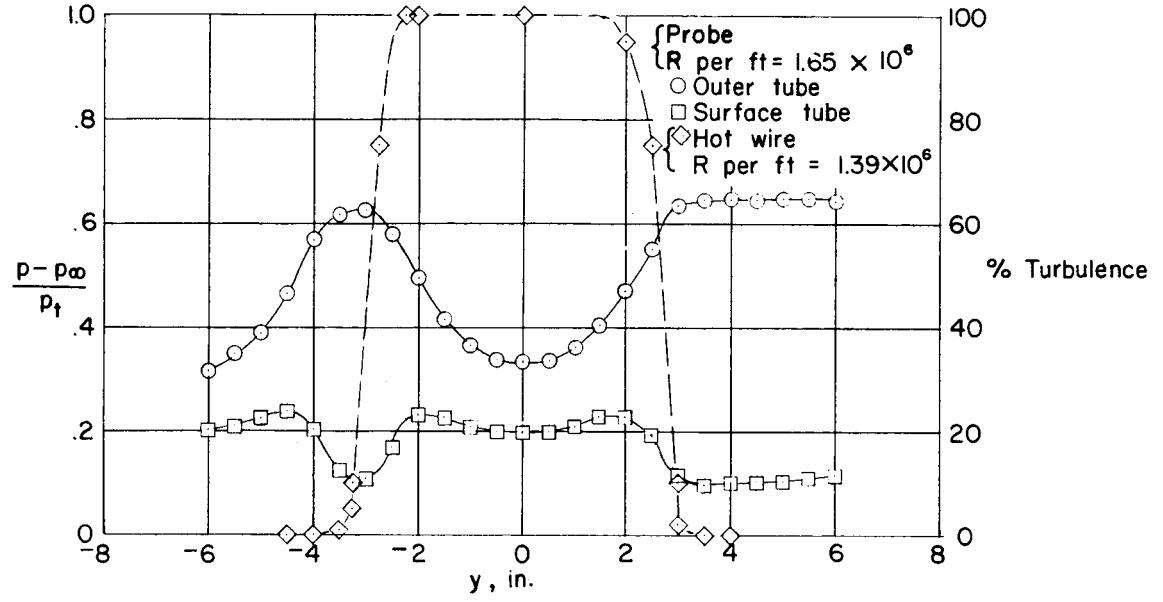

(a) M = 1.61; k = 0.019 at x = 8 inches and y = 0 inch.

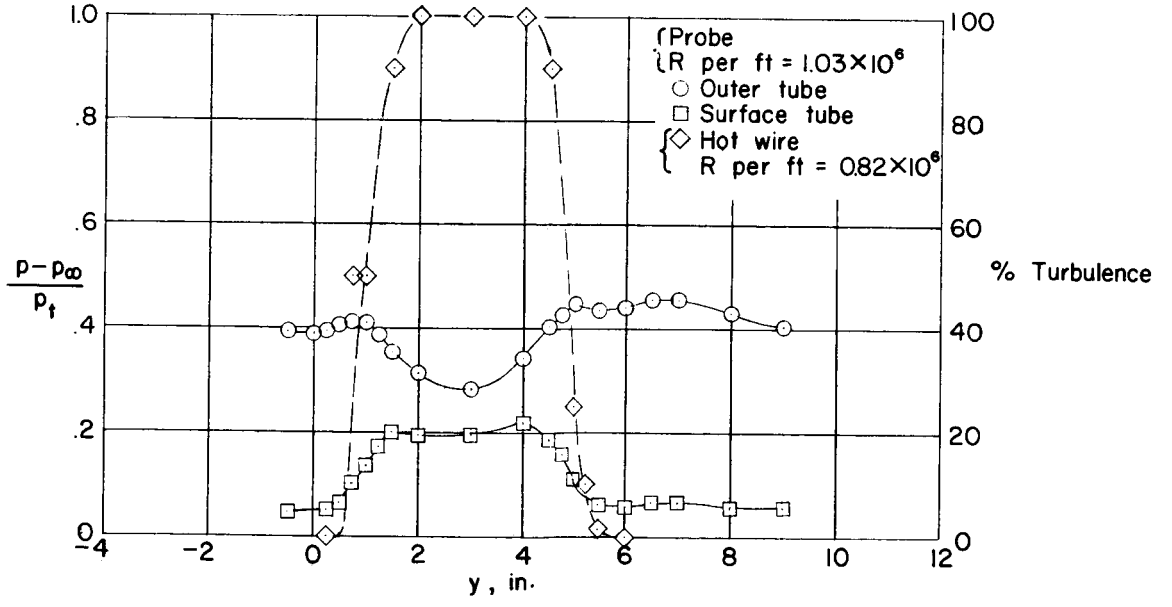

(b) M = 2.01; k = 0.031 at x = 8 inches and y = 3 inches.

Figure 11.- Lateral spread of turbulence behind single-element three-dimensional roughness as determined by total-pressure probe and hot-wire techniques.

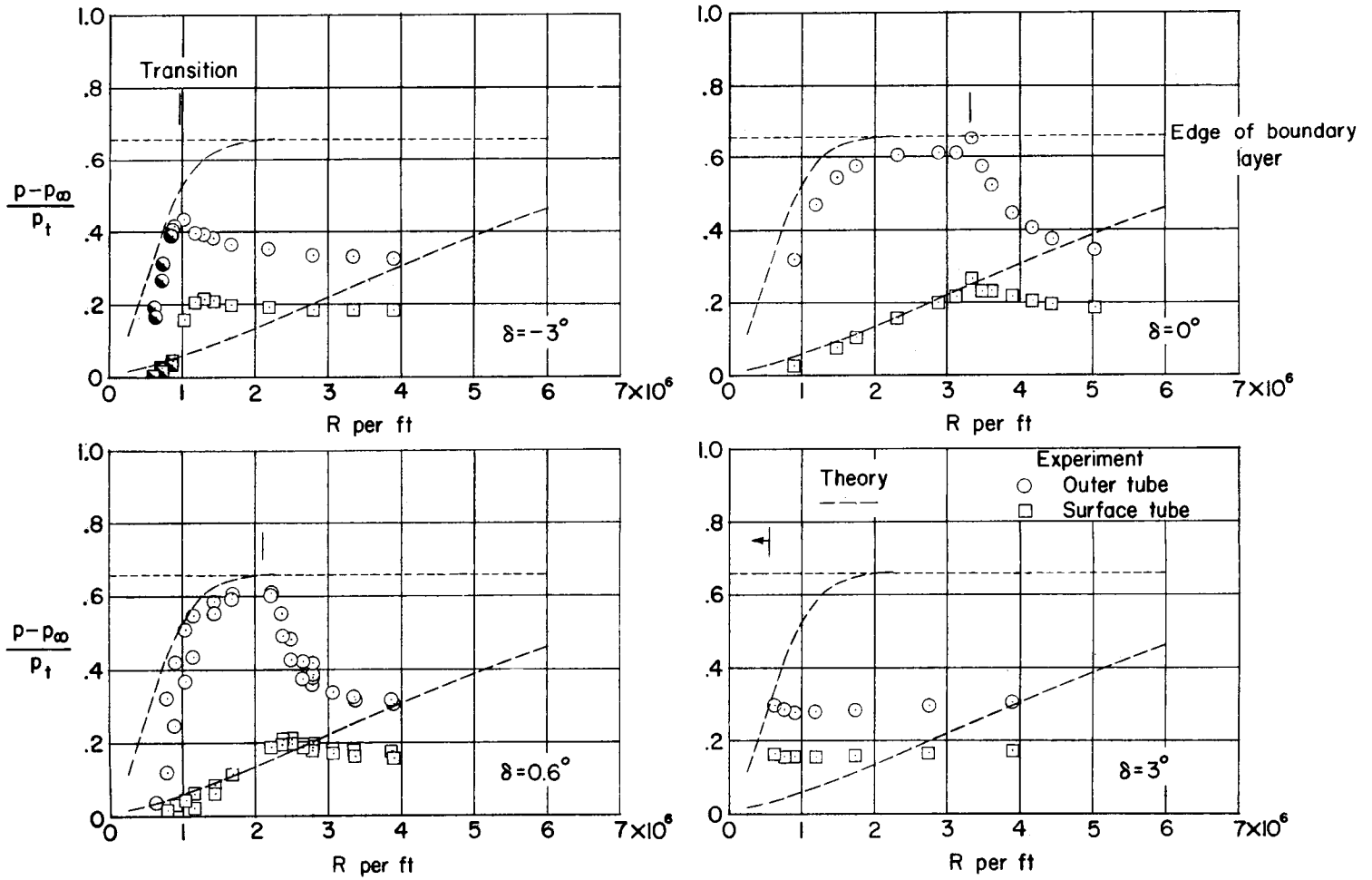

(a) Wedge in forward location.

Figure 12.- Effect of varying Reynolds number per foot on the boundary-layer probe pressures at a station near tunnel center line with wedge installed. M = 1.61. Partially filled symbols indicate an interrupted run.

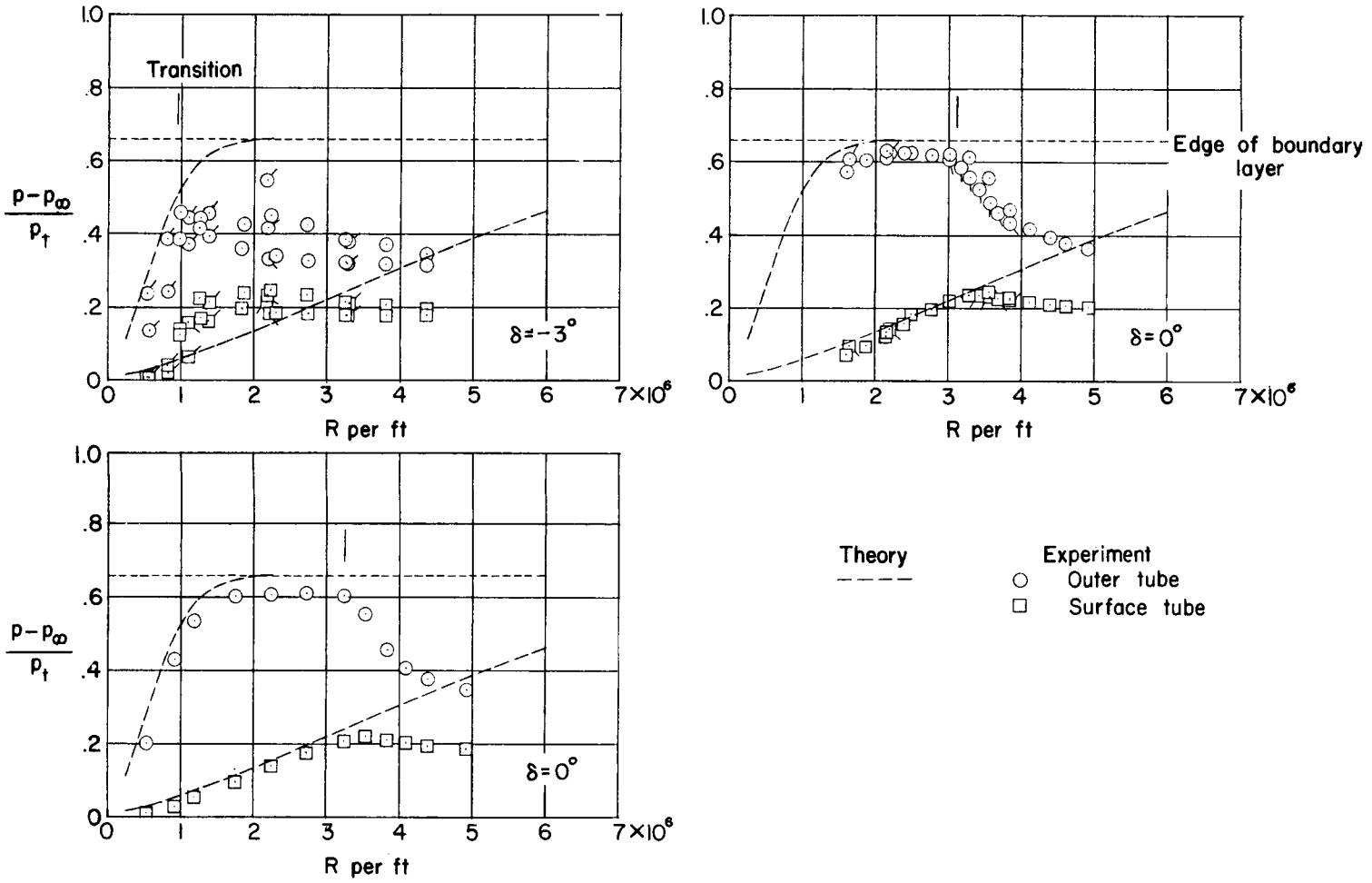

(b) Wedge in middle location.

Figure 12.- Continued.

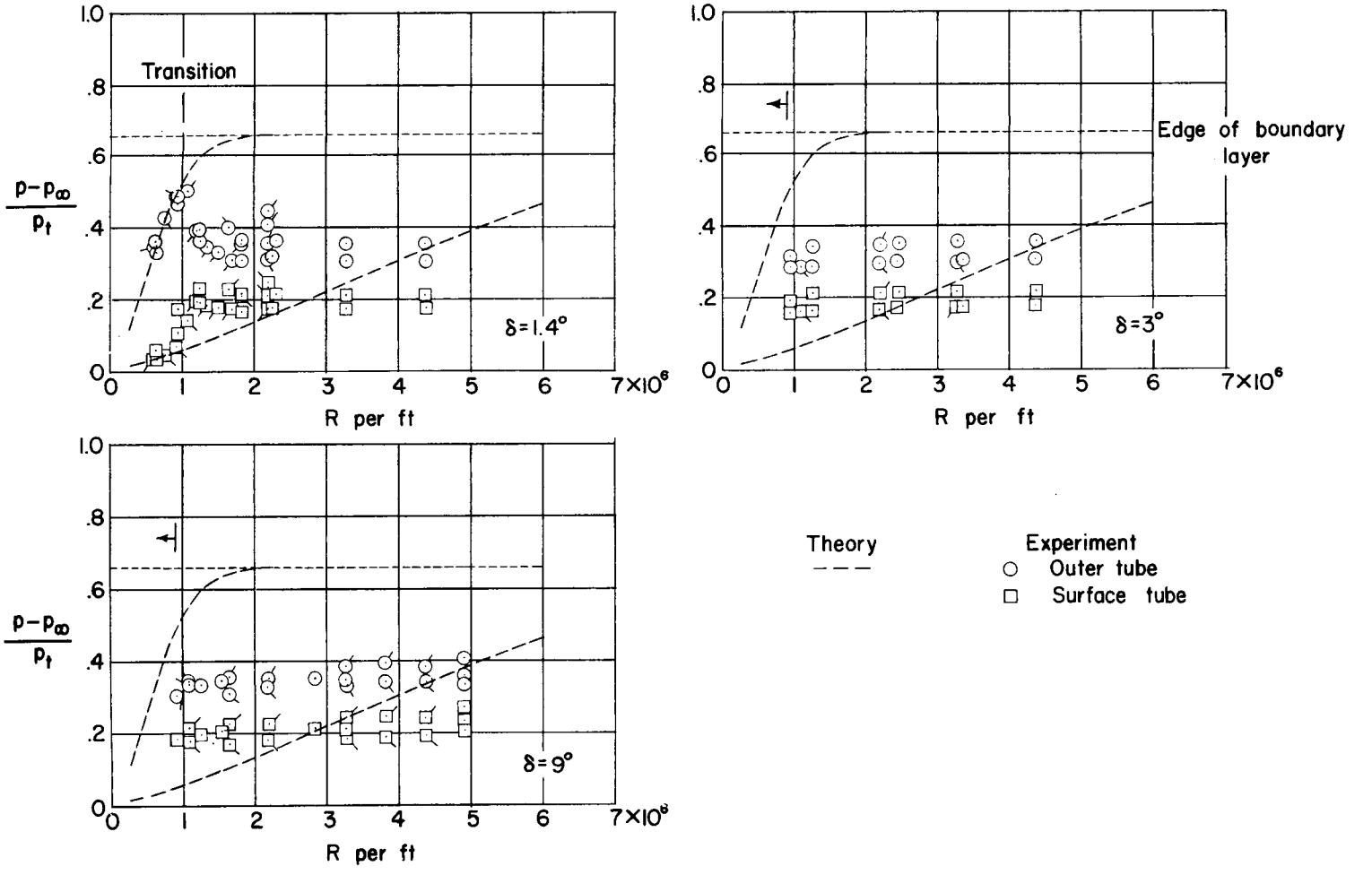

(b) Concluded.

Figure 12.- Continued.

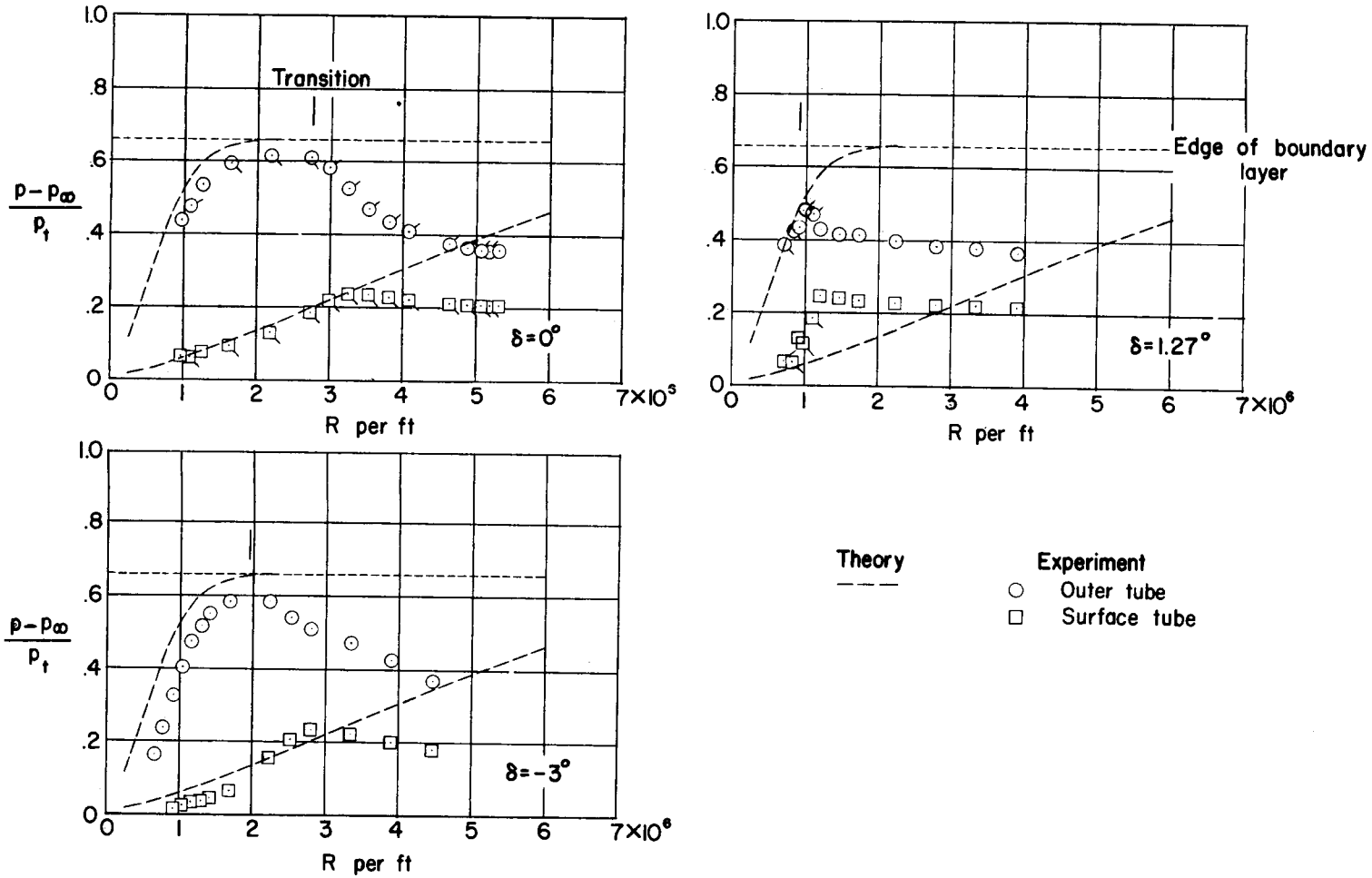

(c) Wedge in rearward location.

Figure 12.- Concluded.

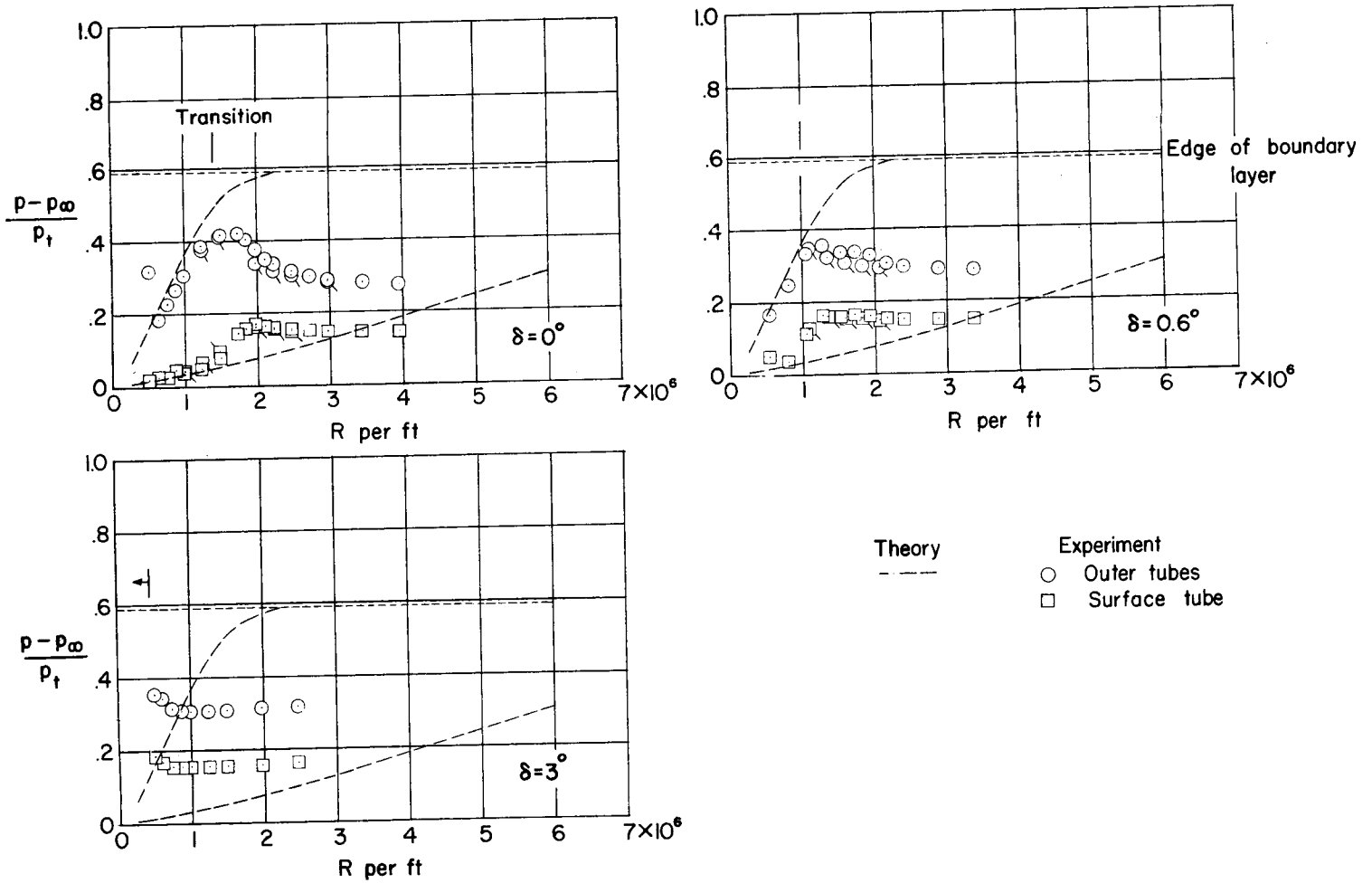

(a) Wedge in forward location.

Figure 13.- Effect of varying Reynolds number per foot on the boundary-layer probe pressures at a station near tunnel center line with wedge installed. M = 2.01.

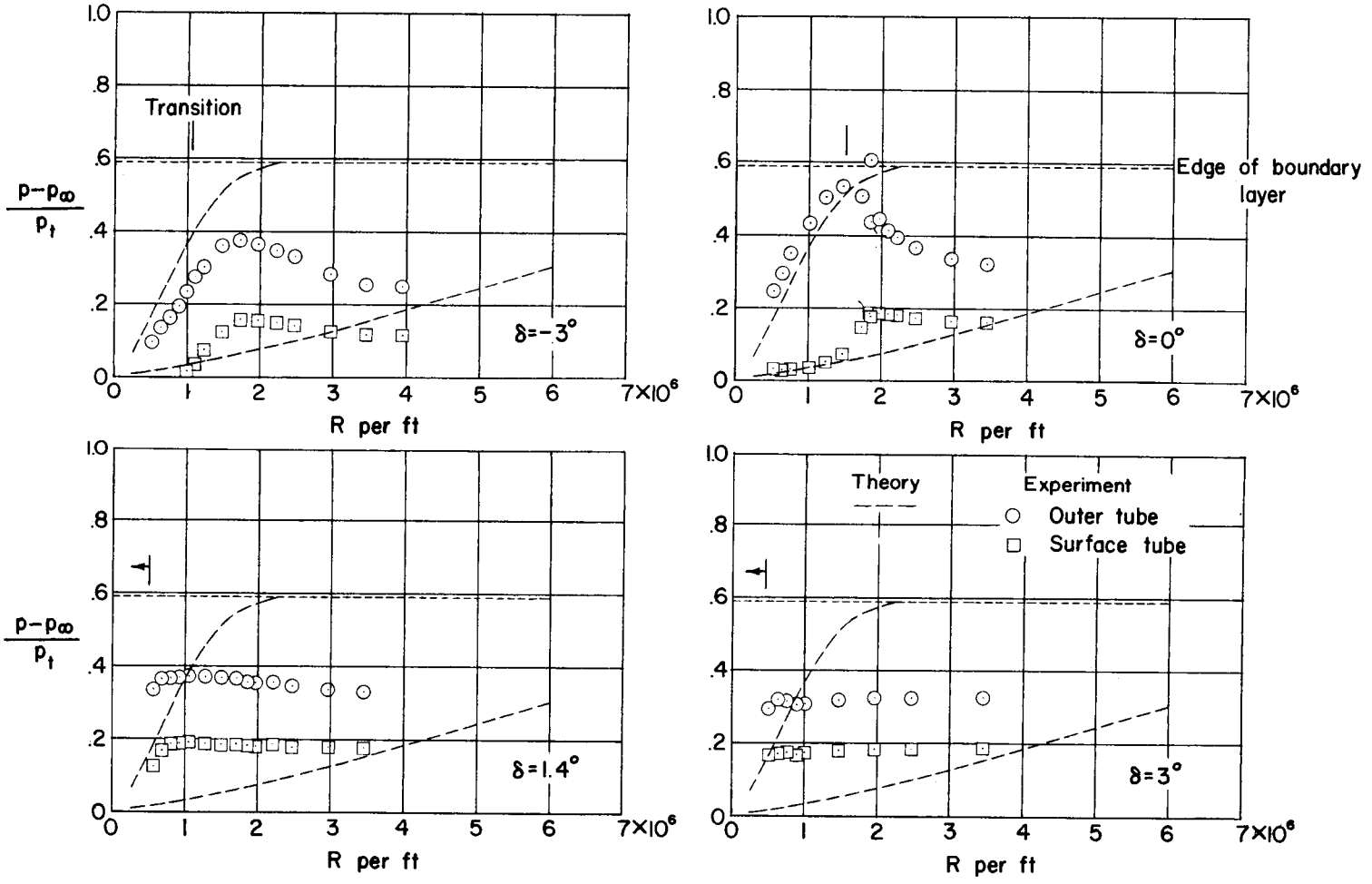

(b) Wedge in middle location.

Figure 13.- Continued.

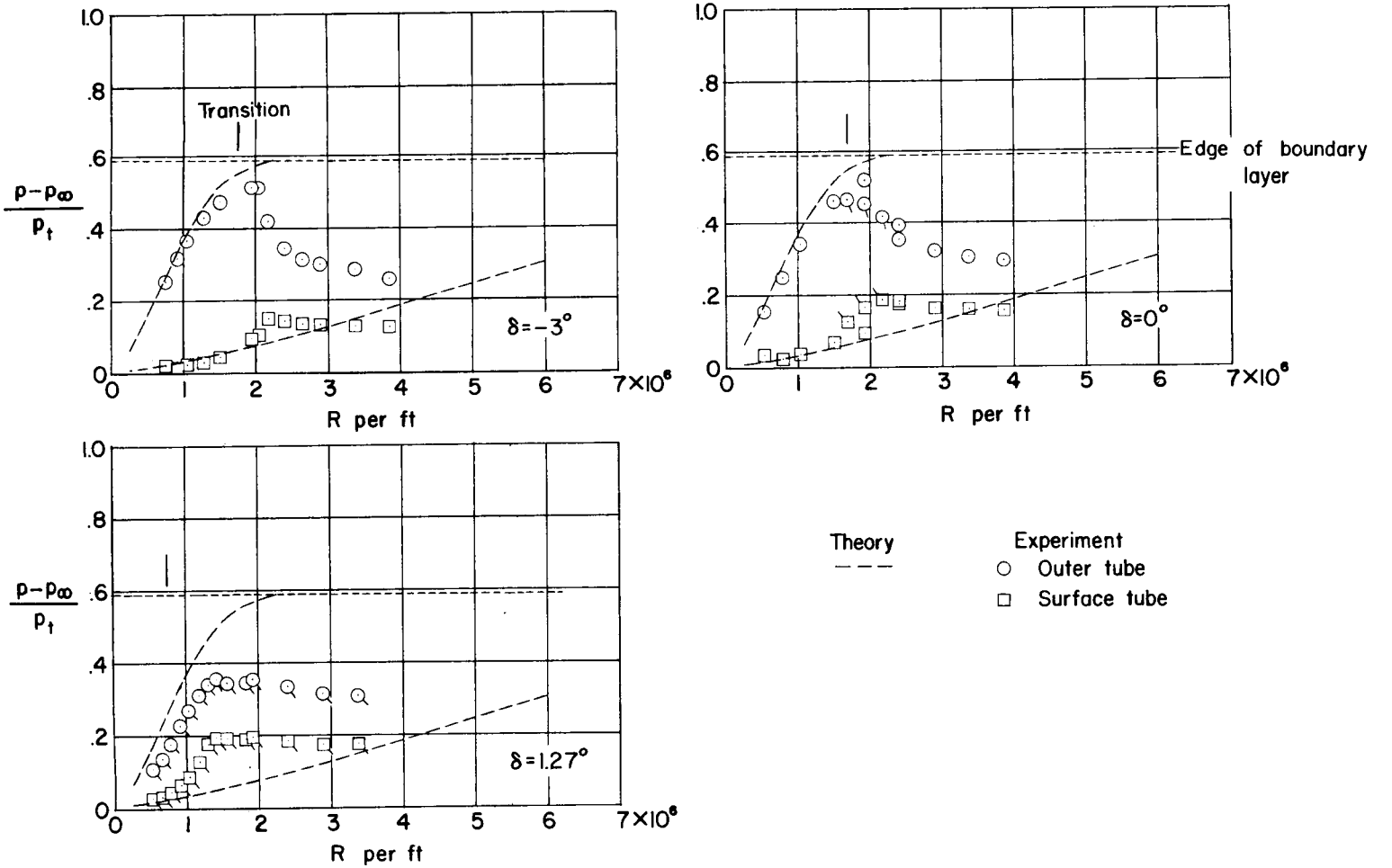

(c) Wedge in rearward location.

Figure 13.- Concluded.

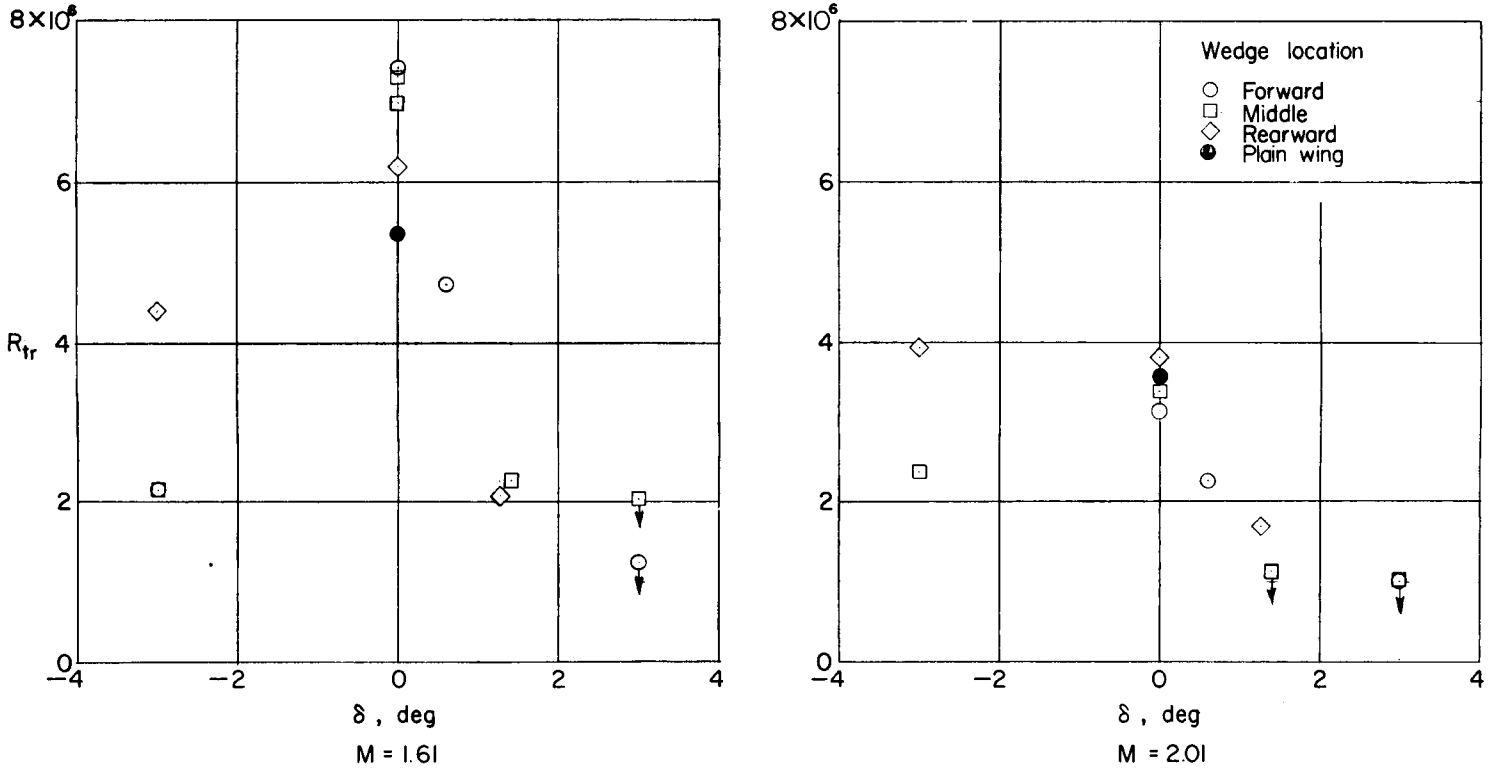

Figure 14.- Effect of varying wedge deflection angle and forward and rearward location on boundary-layer transition Reynolds number at a station near tunnel center line.

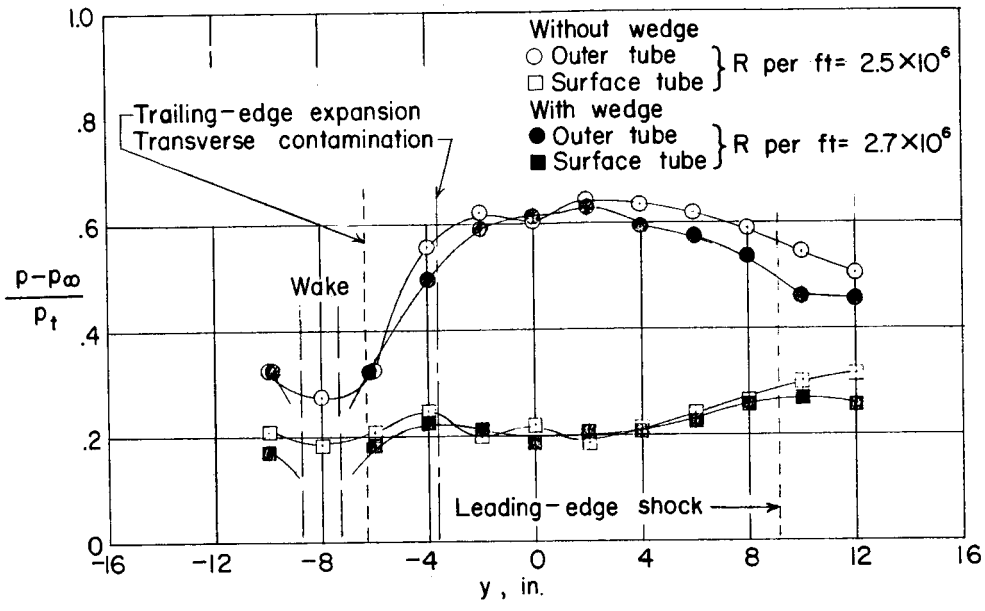

(a) $\delta = 0^{\circ}$.

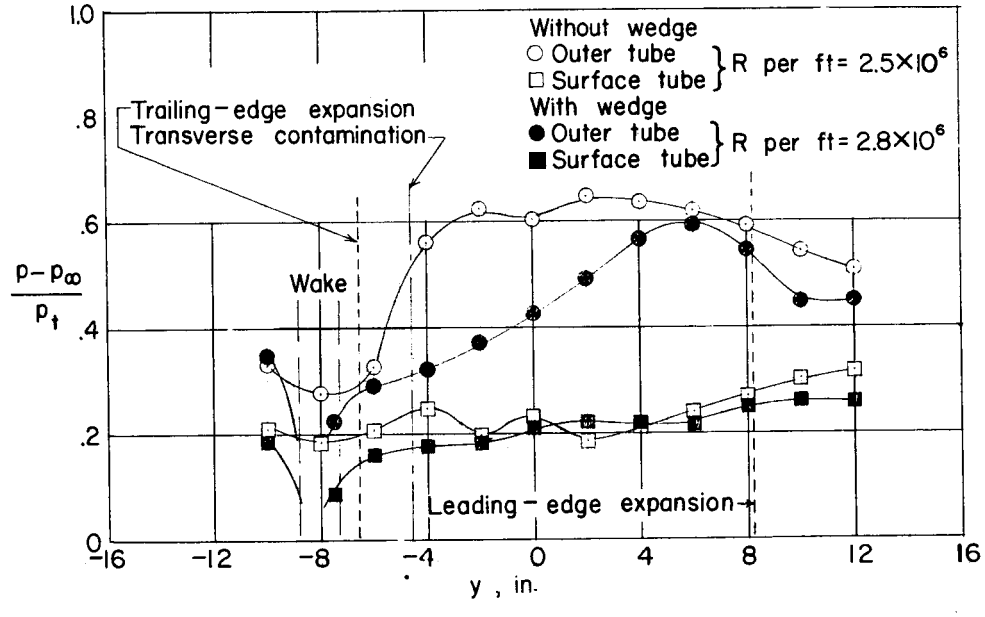

(b) $\delta = -3^{\circ}$.

Figure 15.- Effect of installing wedge on spanwise distribution of boundary-layer probe pressure. M = 1.61; wedge in rearward location.

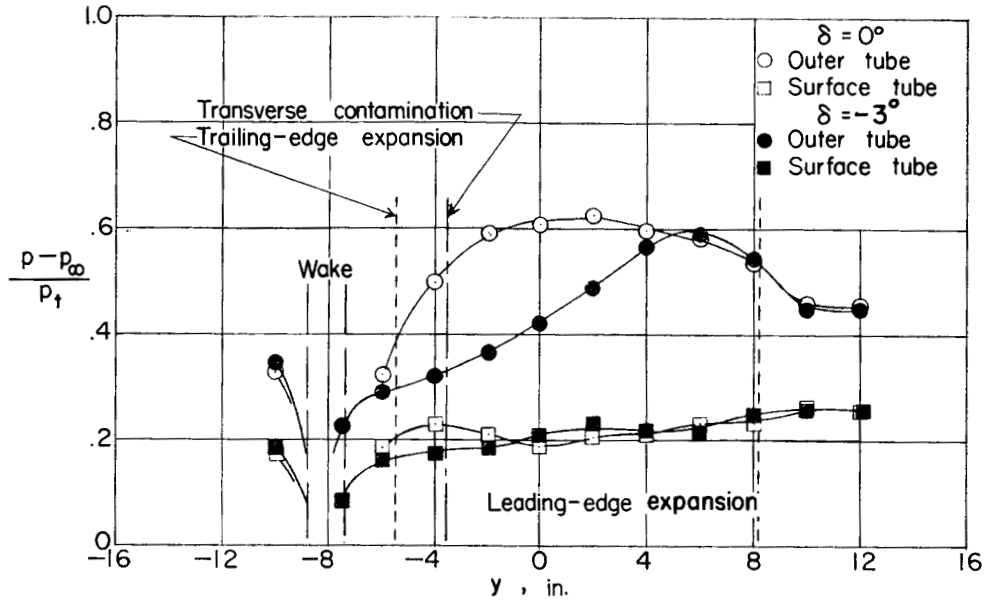

(a) Effect of varying δ, Reynolds number per foot = 2.8×10^6.

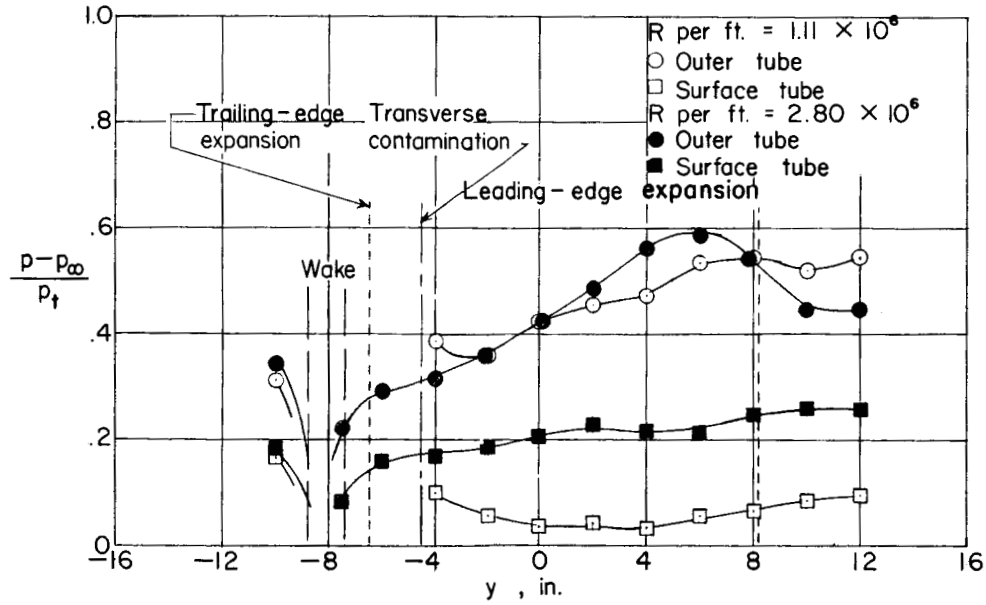

(b) Effect of varying Reynolds number per foot, δ = -3°.

Figure 16.- Effect of varying wedge angle and Reynolds number per foot on the spanwise distribution of boundary-layer probe pressures. M = 1.61; wedge in rearward location.

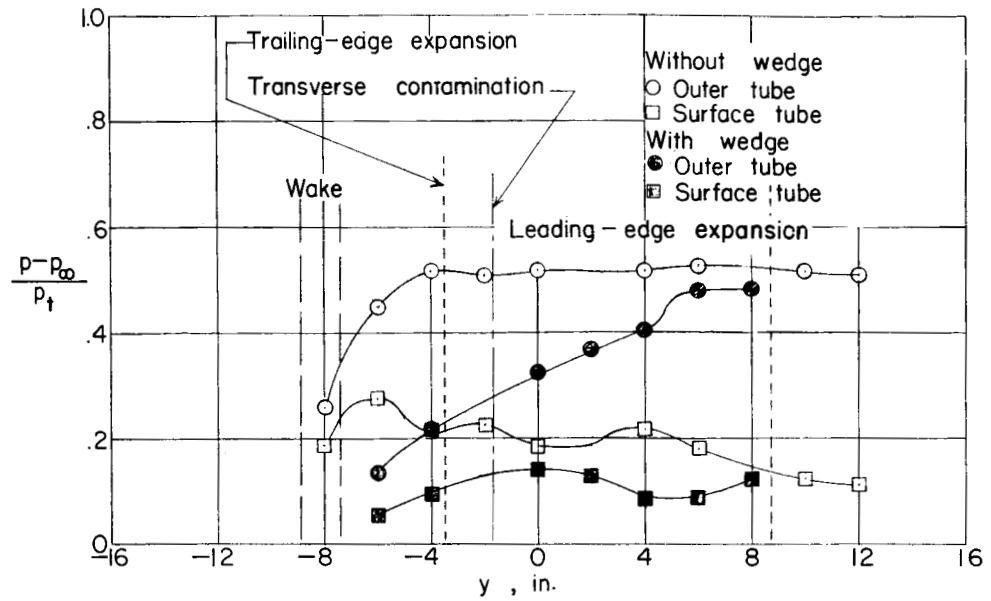

(a) $\delta = -3^\circ$.

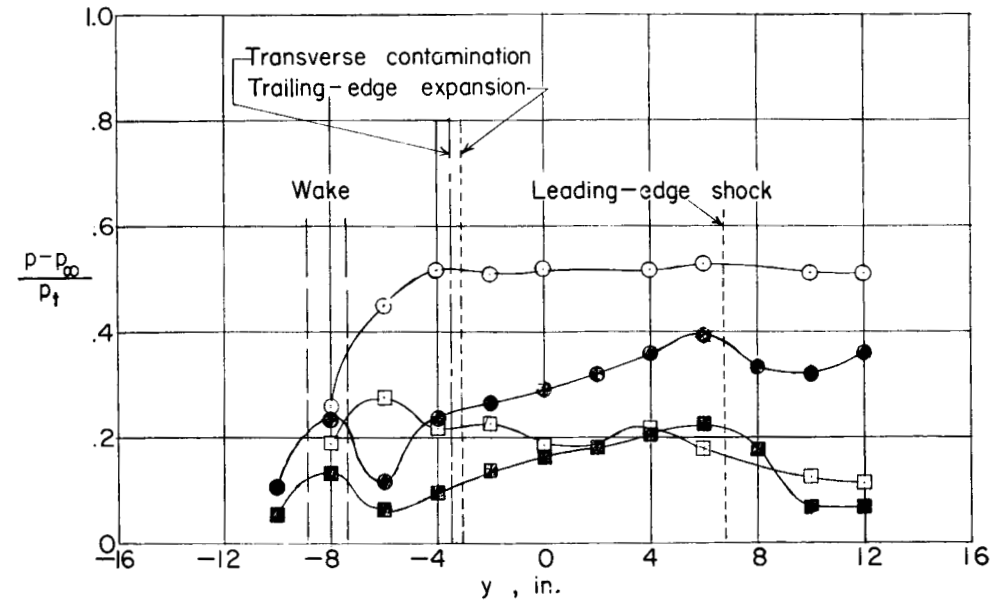

(b) $\delta = 3^\circ$.

Figure 17.- Effect of installing wedge on spanwise distribution of boundary-layer probe pressures. M = 2.01; wedge in middle location; Reynolds number per foot = 1.48×10^6.

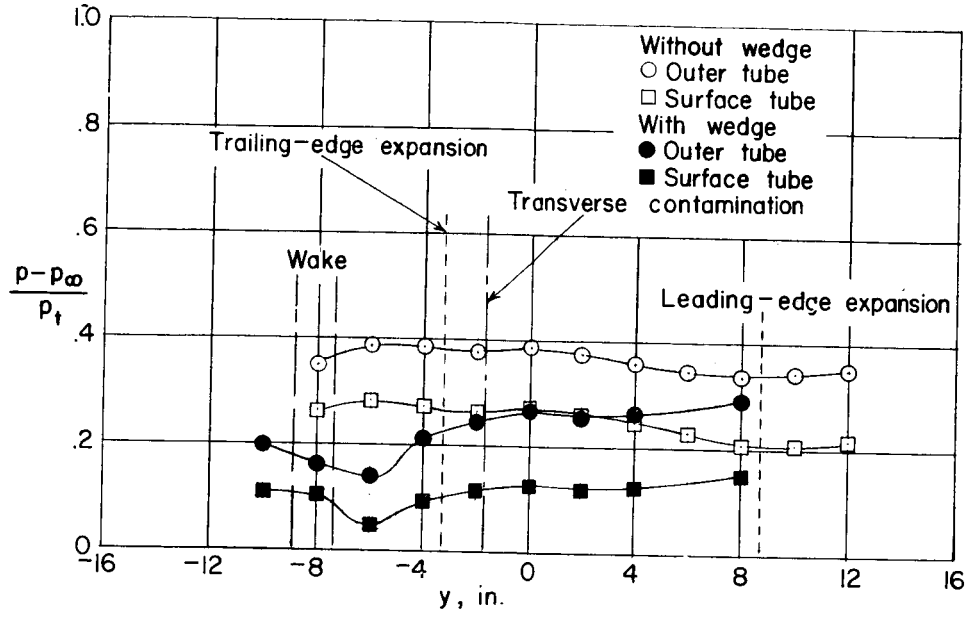

(a) $\delta = -3^\circ$.

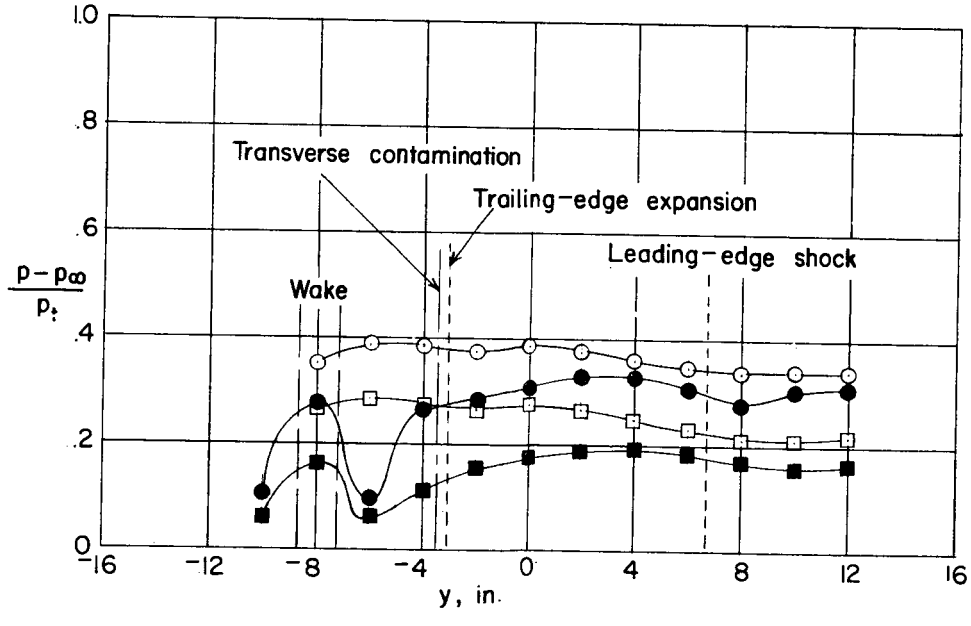

(b) $\delta = 3^\circ$.

Figure 18.- Effect of installing wedge on spanwise distribution of boundary-layer probe pressures. M = 2.01; wedge in middle location; Reynolds number per foot = 3.45×10^6.

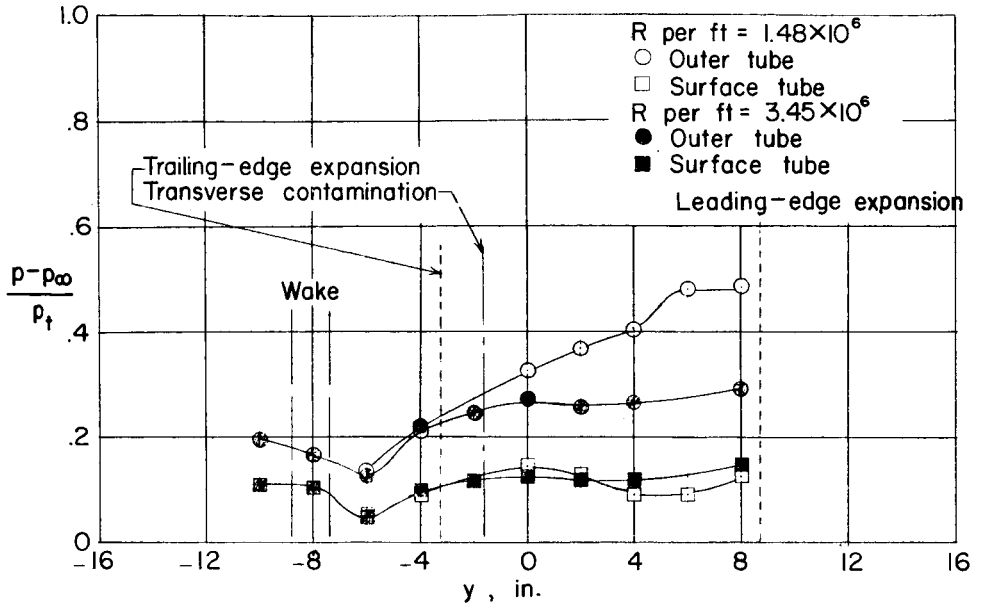

(a) $\delta = -3^{\circ}$.

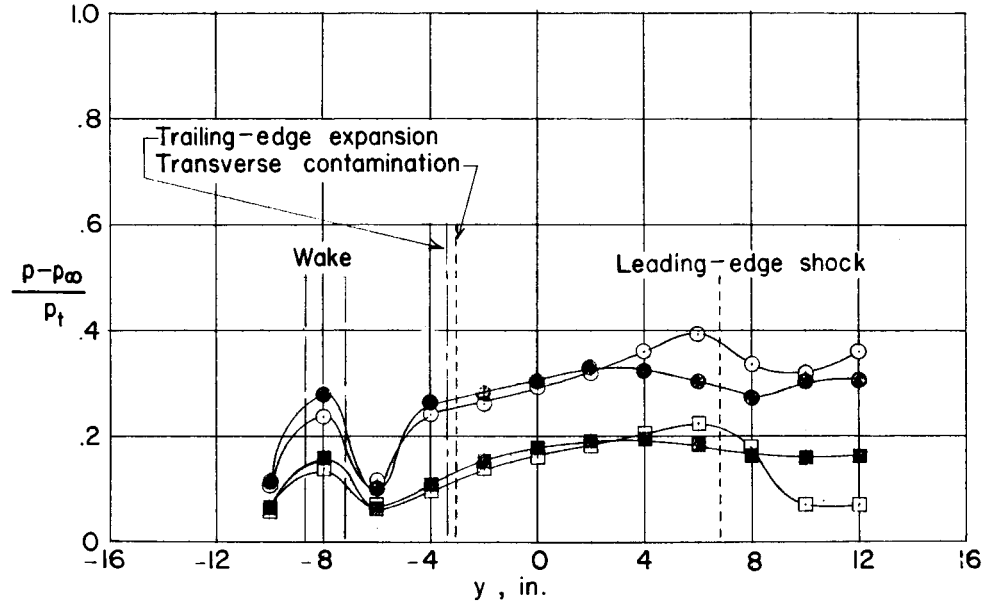

(b) $\delta = 3^{\circ}$.

Figure 19.- Effect of Reynolds number on spanwise distribution of boundary-layer probe pressures. M = 2.01; wedge in middle location.

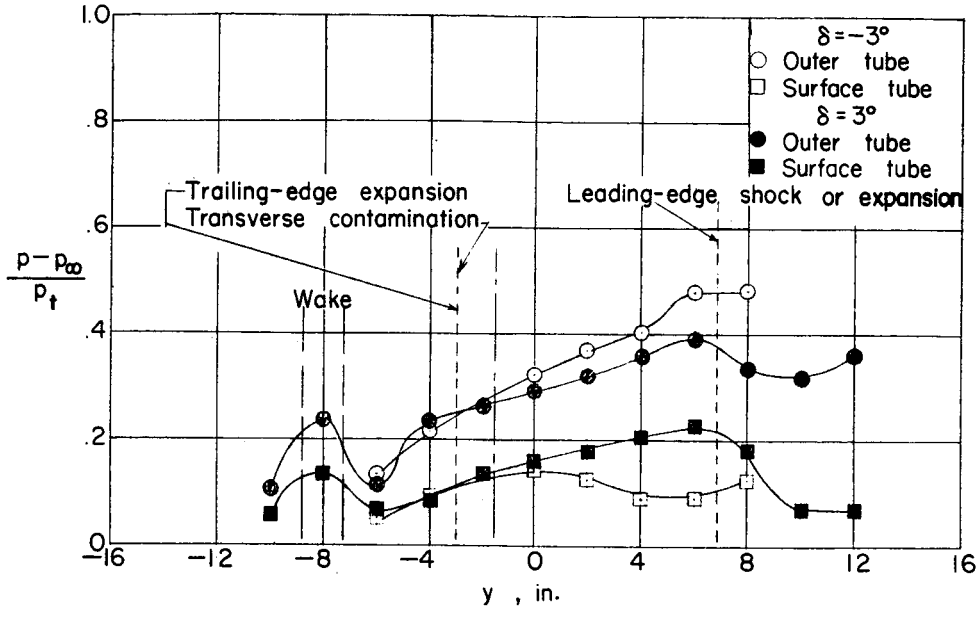

(a) Reynolds number per foot = 1.48×10^6.

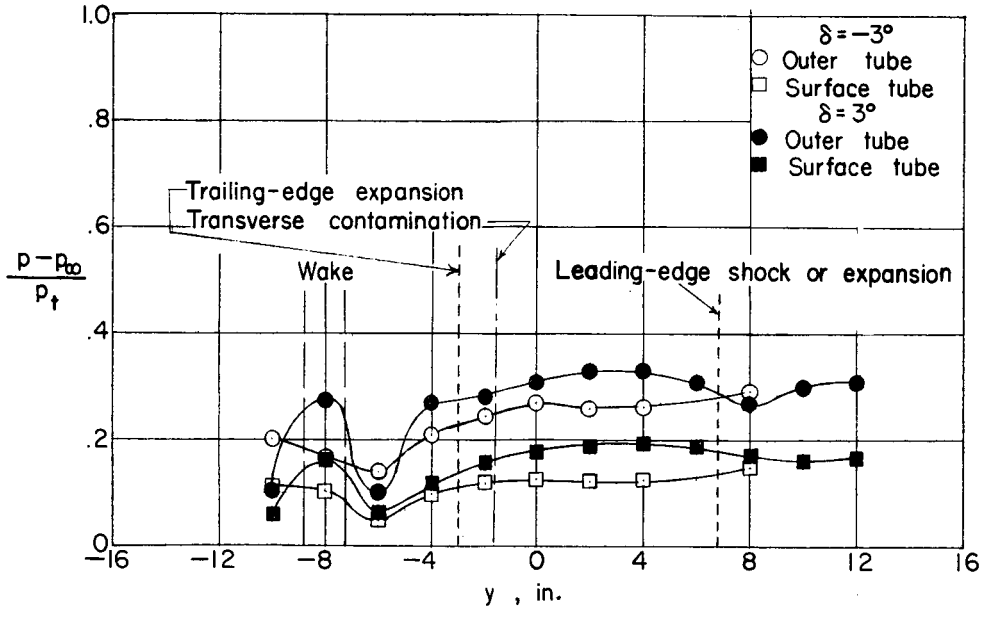

(b) Reynolds number per foot = 3.45×10^6.

Figure 20.- Effect of wedge angle on spanwise distribution of boundary-layer probe pressures. M = 2.01; wedge in middle location.

L-613